Research paper

Two new living Entactinaria (Radiolaria) species from the Arctic province: *Joergensenium arcticum* n. sp. and *Joergensenium clevei* n. sp.

Takahito Ikenoue [a,*], Kjell R. Bjørklund [b], Paulian Dumitrica [c], Anders K. Krabberød [d], Katsunori Kimoto [e], Kohei Matsuno [f], Naomi Harada [e]

[a] Central Laboratory, Marine Ecology Research Institute (MERI), 300 Iwawada, Onjuku-machi, Isumi-gun, Chiba 299-5105, Japan
[b] Natural History Museum, Department of Geology, University of Oslo, P.O. Box 1172, Blindern, 0318 Oslo, Norway
[c] Dennigkofenweg 33, 3073 Guemligen, Switzerland
[d] Section for Genetics and Evolutionary Biology, Department of Biosciences, University of Oslo, P.O box 1066, N-0316 Oslo, Norway
[e] Research and Development Center for Global Change, JAMSTEC, Natsushima-cho 2-15, Yokosuka 237-0061, Japan
[f] Arctic Environment Research Center, National Institute of Polar Research, 10-3 Midori-cho, Tachikawa, Tokyo 190-8518, Japan

ARTICLE INFO

ABSTRACT

Radiolarians in the Arctic Ocean have been studied lately in both plankton and sediment trap samples in the Chukchi Sea area. These studies have shed light on new radiolarian taxa, especially within the order Entactinaria, including two new species of *Joergensenium*, *Joergensenium arcticum* from the western Arctic Ocean, so far restricted to the Pacific Winter Water in the Chukchi Sea, and *Joergensenium clevei* hitherto found in the northern part of the Norwegian Sea south of the Fram Strait. The taxonomic position of the order Entactinaria is discussed and the genus *Joergensenium* has been emended. We have also observed in detail the internal structure of *Joergensenium arcticum* using Microfocus X-ray Computed Tomography and have utilized three-dimensional imaging for the first time in a species description.

© 2016 Elsevier B.V. All rights reserved.

1. Introduction

Radiolarians (siliceous marine Rhizaria) are widely distributed in the oceans throughout the water column from the surface to great depths. Their species-specific abundance in a region is related to temperature, salinity, productivity, and nutrient availability (Anderson, 1983; Bjørklund et al., 1998; Cortese and Bjørklund, 1997; Cortese et al., 2003; Ikenoue et al., 2012a, 2012b, 2015). Therefore, information on the vertical distributions of living radiolarians, their life cycle, and their response to sea-ice reduction can contribute to the historical reconstruction of the vertical hydrographic structure and predict future ecosystems in the Arctic. In the Arctic Ocean, radiolarian assemblages have been studied mainly based on the samples collected by plankton tows and surface sediment samples (Itaki et al., 2003; Bjørklund and Kruglikova, 2003). In recent studies, seasonal and interannual variations of the radiolarian fauna and their relationships with sea-ice and ocean circulation have been carried out using sediment trap and vertical plankton tow samples (Ikenoue et al., 2015). Ikenoue et al. (2015) suggested that the depth distribution of *Joergensenium* sp. A is restricted to the Pacific Winter Water. *Joergensenium* sp. A has not been described yet and has so far only been observed in the Chukchi Sea, in the western part of the Arctic Ocean. So far, we have not observed this species in recent materials outside the Arctic Ocean, neither in the North Pacific nor in the North Atlantic.

In this study, we have observed and documented the skeletal characteristics of *Joergensenium* sp. A, and herein describe it as a new species *Joergensenium arcticum*, including a discussion of its vertical distribution, life cycle, symbionts and parasites in the Arctic Ocean. Furthermore we have observed other Entactinarian species in the material we have available. On Cleve slide #33 (P.T. Cleve's type collection, Swedish Museum of Natural History) two specimens of a new species have been described as *Joergensenium clevei*.

2. Regional setting

The oceanography of the Arctic is characterized by strong stratification and limited connections with the Pacific, enormous continental shelves, sea-ice formation and melting. A clear decreasing trend in sea-ice extent has been observed in the Arctic Ocean since the 2000s (Stroeve et al., 2012). The most rapid reduction of sea ice has been observed in the western Arctic Ocean (Comiso, 2012), which has a higher

rate of primary production than any other area of the Arctic Ocean owing to the supply of nutrient-rich Pacific water (Harada, 2016). The hydrography in the western Arctic Ocean has been discussed in several studies (e.g., Aagaard et al., 1985; McLaughlin et al., 2011). The surface water is characterized by low-temperature and low salinity water and all of the deep water is supplied by dense, saline water from the Atlantic Ocean (Aagaard et al., 1981). The surface water can be subdivided into three layers, i.e., surface mixed layer (SML), Pacific Summer Water (PSW), and Pacific Winter Water (PWW). The SML (0–25 m) is formed in summer by sea-ice melt and river runoff, and is characterized by low salinities (less than 28). The PSW (25–100 m) and PWW (100–250 m) are cold, halocline layers originating from the Pacific Ocean via the Bering Sea. The Pacific water enters through the very shallow Bering Strait (~50 m sill depth). The PSW is relatively warmer and less saline (30–32 in the 1990s, 28–32 in the 2000s) than the PWW (Jackson et al., 2011). The PWW is characterized by a temperature minimum (of about −1.7 °C) (Coachman and Barnes, 1961) and a nutrient maximum (Jones and Anderson, 1986).

3. Material and methods

3.1. Plankton tow samples

Plankton tow samples were collected from the northern Chukchi Sea using vertical tows with a NORPAC net (North Pacific standard plankton net) (62-μm mesh size, open mouth area: 0.16 m²) and a vertical multiple plankton sampler (VMPS) (62-μm mesh size, open mouth area: 0.25 m²) to elucidate the relationships between radiolarians and the vertical hydrographic structure. Plankton tow samples were also collected from the Bering Strait and the southern Chukchi Sea using vertical tows with a NORPAC net to investigate the amount of radiolarians

drifting from the Bering Sea to the western Arctic Ocean. The VMPS was towed from four layers (100–0, 250–100, 500–250, and 1000–500 m) at two stations (Station 32 and Station 56 in the northern Chukchi Sea) in September 2013 (Fig. 1, Table 1).

During August–October 2013 the NORPAC net was towed from 150 m depth to the surface. At 9 stations the depths were shallower than 150 m and the towing started 5 m above actual bottom depth (Stations 1 and 3 in the Bering Strait; Stations 5, 7, 8, 9, 68, 70 in the southern Chukchi Sea; Station 52 in the northern Chukchi Sea) (Fig. 1, Tables 1 and 2). The volume of seawater filtered through the net was estimated using a flow meter mounted in the mouth of the net. Hydrographical data (temperature, salinity, dissolved oxygen, and chlorophyll *a*) down to 1000 m water depth were simultaneously obtained from CTD (Conductivity Temperature Depth profiler) casts. The samples collected by NORPAC net and VMPS were split with a Motoda box splitter and a rotary splitter (McLane™WSD-10). The split samples were fixed with 99.5% ethanol for microscopic observation and molecular analysis.

Plankton samples from the northern Chukchi Sea were stained with Rose-Bengal to discriminate between living and dead specimens. Specimens that clearly stained bright red were interpreted as living cells, while cells that did not stain red, or were just barely stained red, were interpreted as dead because they lacked sufficient intact protoplasm to absorb the stain. Plankton samples from the Bering Strait and southern Chukchi Sea were treated with the same method as for the sediment trap samples described by Ikenoue et al. (2015) to remove organic matter and more easily identify the presence of radiolarian skeletons. Plankton tow sample slides for light microscope observation were prepared using the methods described by Ikenoue et al. (2015). We counted all specimens encountered on each slide with an Olympus BX43 transmitted light microscope at 200× or 400× magnification, and
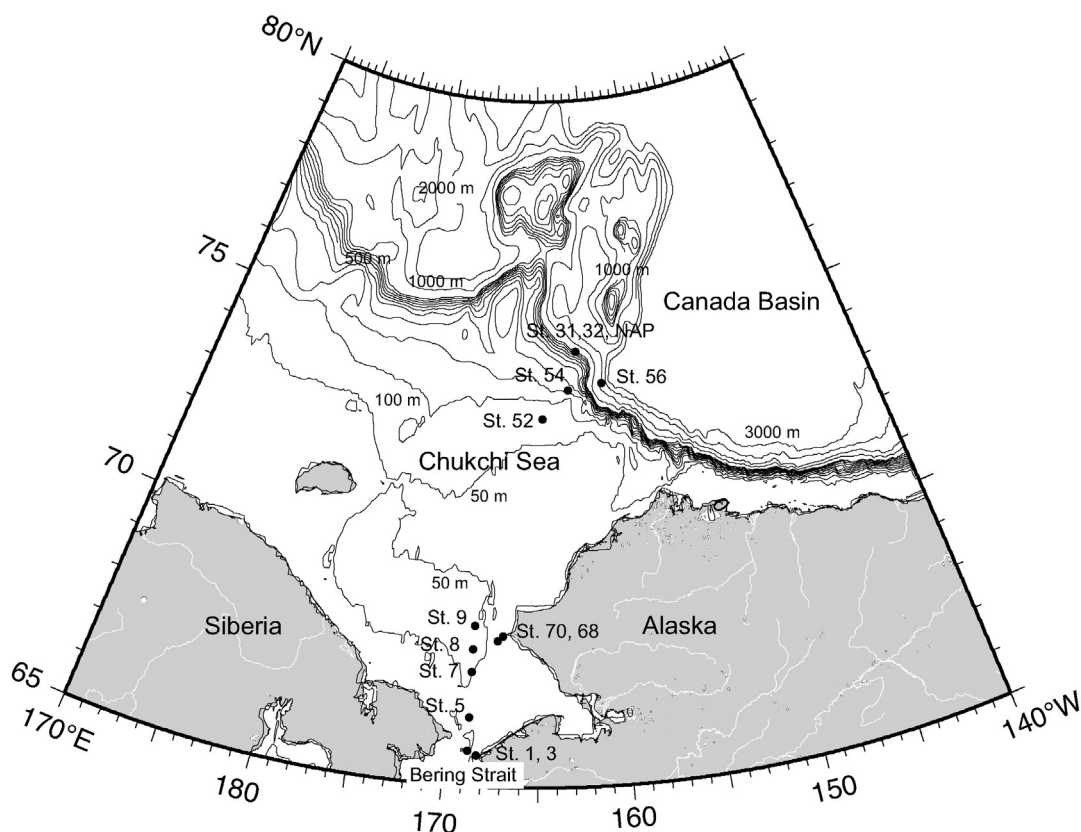

Fig. 1. Location map of sampling stations in the northern Chukchi Sea, southern Chukchi Sea, and Bering Strait.

Table 1
Logistic and sample information for the vertical plankton tows for *Joergensenium arcticum* standing stock (S. S.) at five stations in the northern Chukchi Sea during R/V Mirai Cruise MR13-06.

Station ID / Date	Sampling time (UTC)	Depth interval (m)	Flow water mass (m³)	Aliquot size	Living *J. arcticum* Adult S.S. (count)	Juvenile S.S. (count)	Total[a] S.S. (count)	2 conjoined S.S. (count)	3 conjoined S.S. (count)	Dead *J. arcticum* Adult S.S. (count)	Juvenile S.S. (count)	Total[a] S.S. (count)	2 conjoined S.S. (count)	3 conjoined S.S. (count)
Station 31 74°32′N, 161°54′W 08 Sep. 2013	7:07	0–150	11.0	1/20	11.0 (6)	7.3 (4)	18.3 (10)	0 (0)	0 (0)	5.5 (3)	1.8 (1)	7.3 (4)	0 (0)	0 (0)
Station 32 74°32′N, 161°54′W 09 Sep. 2013	1:24	0–100	20.4	1/4	0 (0)	0 (0)	0 (0)	0 (0)	0 (0)	0 (0)	0 (0)	0 (0)	0 (0)	0 (0)
	1:22	100–250	27.2	1/4	16.9 (115)	3.5 (24)	20.4 (139)	0.9 (6)	0 (0)	1.8 (12)	0.9 (6)	2.6 (18)	0 (0)	0 (0)
	1:18	250–500	39.7	1/2	0.8 (15)	0.1 (2)	0.9 (17)	0 (0)	0 (0)	2.3 (46)	0.2 (4)	2.5 (50)	0 (0)	0 (0)
	1:10	500–1000	79.3	1/2	0.1 (4)	0 (0)	0.1 (4)	0 (0)	0 (0)	0.5 (19)	0.1 (2)	0.5 (21)	0 (0)	0 (0)
Station 52 73°04′N, 164°37′W 26 Sep. 2013	22:45	0–66	5.0	1/10	0 (0)	0 (0)	0 (0)	0 (0)	0 (0)	0 (0)	0 (0)	0 (0)	0 (0)	0 (0)
Station 54 73°42′N, 162°39′W 27 Sep. 2013	5:11	0–150	11.2	1/10	21.4 (24)	15.2 (17)	36.6 (41)	0.9 (1)	0 (0)	0 (0)	0 (0)	0 (0)	0 (0)	0 (0)
Station 56 73°48′N, 159°59′W 27 Sep. 2013	14:00	0–150	12.5	1/20	9.6 (6)	12.8 (8)	22.5 (14)	0 (0)	0 (0)	1.6 (1)	8 (5)	9.6 (6)	0 (0)	0 (0)
Station 56 73°48′N, 159°59′W 27 Sep. 2013	17:36	0–100	15.8	1/4	0 (0)	0 (0)	0 (0)	0 (0)	0 (0)	1 (4)	0 (0)	1.0 (4)	0 (0)	0 (0)
	17:34	100–250	23.8	1/2	20.7 (246)	7.6 (91)	28.3 (337)	0.5 (6)	0.1 (1)	1.2 (14)	0.8 (9)	1.9 (23)	0 (0)	0 (0)
	17:30	250–500	40.8	1/2	2.6 (53)	0.7 (14)	3.3 (67)	0 (0)	0 (0)	17.2 (351)	1.7 (34)	18.9 (385)	0.2 (3)	0 (0)
	17:22	500–1000	81.8	1/2	0 (1)	0 (1)	0.1 (2)	0 (1)	0 (0)	4.1 (166)	1.2 (49)	5.3 (215)	0 (0)	0 (0)

[a] Counts of 2 and 3 conjoined are divided between counts of adult and juvenile.

defined the two-shelled form of *J. arcticum* as a juvenile. The individual numbers of counted specimens were converted to standing stocks (No. of specimens m^{-3}).

The split specimens were also observed with a scanning electron microscope (SEM): JSM-6700F (JEOL, Tokyo, Japan) and by Microfocus X-ray Computed Tomography (MXCT): ScanXmate-DF160TSS105 (Comscantechno co.ltd, Shinyokohama, Japan) with a high-resolution X-ray detector (spatial resolution: 0.8 μm/voxel) for detailed description of the skeletal structure of *J. arcticum*. Microfocus X-ray Computed Tomography is a non-destructive three-dimensional (3D) imaging technique. The 3D image of the interior of an object is obtained by collecting X-ray transmission images from whole angles and generating a series of two-dimensional cross-sectional images. These two-dimensional images are stacked and a 3D image is built using computer software. We visualized the CT-scanned 3D images of *J. arcticum* (Appendix A) by 3D image viewer "Molcer Plus" (http://www.white-rabbit.jp/molcerPlusE.html).

The methods used for analyzing the symbionts of *J. arcticum* follows the same protocol as Krabberød et al. (2011) and Bråte et al. (2012). Plankton samples for molecular analysis were preserved in 70% ethanol until further processed. In the lab, individual cells of *J. arcticum* were isolated by capillary isolation and washed by physically removing external debris with microneedles. Then, each cell was rinsed in three droplets of sterile filtered Milli-Q water, and transferred into 200 μl PCR-tubes. Single cell whole genome amplification (SCWGA), 18S PCR and ABI sequencing with general eukaryotic primers was performed as in Bråte et al. (2012).

Obtained sequences were added to a reference alignment of the major groups of dinoflagellates (Orr et al., 2012) combined with an alignment of representatives of marine alveolates (MALV) (Guillou et al., 2008; Bråte et al., 2012) and the nearest BLAST-hits in GenBank. The sequences were aligned with MAFFT v7.017 (Katoh and Standley, 2013) implemented in Geneious 8, and then trimmed with trimAL with automated settings (Capella-Gutiérrez et al., 2009). The resulting alignment had 308 taxa and 1471 characters. Maximum likelihood analysis was performed with the program RAxML v8.0.26 using the rapid bootstrapping and subsequent ML search with the GTRGAMMA model. The number of bootstraps was automatically set based on the MRE bootstopping criterion (Stamatakis, 2014) and stopped at 350 replicates. Ten sequences obtained from *J. arcticum* fell within MALV (not shown). To further determine the placement of the sequences from *J. arcticum*, the distantly-related clades were removed and a new phylogenetic analysis was performed on the reduced dataset (89 taxa, 1495 characters) following the same routine as described before. Sequences used in this study have been deposited in NCBI GenBank (http://www.ncbi.nlm.nih.gov/) with accession numbers KT751274-KT751283.

3.2. Sediment trap samples

Sinking particles were collected by a sediment trap (SMD26 S-6000, open mouth area 0.5 m², Nichiyu Giken Kogyo, Co. Ltd.) with bottles rotating at intervals of 10–15 days, and the trap moored at 184 m (4th October 2010–28th September 2011), and 260 m (4th October 2011–18th September 2012), and a second trap moored at 1300 m (4th October 2010–28th September 2011), and 1360 m (4th October 2011–18th September 2012) at Station NAP on the Northwind Abyssal Plain (Fig. 1, Table 3). Recoveries and redeployments of the traps were carried out by the ice breaker of the Canadian Coast Guard I/B "Sir Wilfrid Laurier" and the R/V "Mirai" of the Japan Agency for Marine-Earth Science and Technology.

Sediment trap sample slides for light microscope observation were prepared using the methods described by Ikenoue et al. (2015). We counted all *J. arcticum* skeletons encountered on each slide with an Olympus BX43 transmitted light microscope at 200× or 400× magnification and defined the two-shelled form of *J. arcticum* as a juvenile. The

Table 2
Logistic and sample information for the vertical plankton tows for radiolarian standing stock (S. S.) at eight stations in the southern Chukchi Sea and Bering Strait during R/V Mirai Cruise MR13-06.

Station ID		Sampling time (UTC)	Depth interval (m)	Flow water mass (m³)	Aliquot size	Total radiolarian S. S. (count)	Temperature range (°C)	Salinity range
Station 1	65°46′ N, 168°45′W	19:28	0–45	2.42	1/32	0 (0)	1.21–6.87	31.39–32.28
Date	31 Aug. 2013							
Station 3	65°41′ N, 168°17′W	23:38	0–38	3.81	1/32	0 (0)	5.90–11.19	24.64–31.40
Date	31 Aug. 2013							
Station 5	66°30′ N, 168°45′W	5:10	0–48	1.24	1/32	0 (0)	2.05–7.54	31.22–32.11
Date	01 Sep. 2013							
Station 7	67°30′ N, 168°45′W	11:41	0–42	2.83	1/32	0 (0)	1.08–5.88	31.64–32.35
Date	01 Sep. 2013							
Station 8	68°00′ N, 168°45′W	18:10	0–52	3.60	1/32	0 (0)	2.23–5.05	32.11–32.42
Date	01 Sep. 2013							
Station 9	68°30′ N, 168°45′W	22:46	0–46	4.00	1/16	0 (0)	2.26–7.86	29.66–32.05
Date	09 Sep. 2013							
Station 68	68°18′ N, 167°03′W	23:59	0–31	2.81	1/8	5.7 (2)	4.58–6.03	30.13–31.62
Date	02 Oct. 2013							
Station 70	68°12′ N, 167°20′W	2:04	0–40	3.44	1/8	2.3 (1)	3.34–4.63	30.19–31.82
Date	03 Oct. 2013							

flux of _J. arcticum_ (No. of specimens m^{-2} day^{-1}) was calculated from count data using the following formula:

$$Flux = N * V/S/D \qquad (1)$$

where _N_ is the counted number of radiolarians, _V_ the aliquot size, _S_ the aperture area of the sediment trap (0.5 m²), and _D_ the sampling interval (day).

As supplemental environmental data, Time-series data of sea-ice concentration around Station NAP during the mooring period were calculated from the sea-ice concentration data set (http://iridl. ldeo. columbia.edu/SOURCES/.IGOSS/.nmc/.Reyn_Smith OIv2/, cf. Reynolds et al., 2002).

4. Results

4.1. Taxonomy

Infrakingdom Rhizaria Cavalier-Smith, 2002, emend. Cavalier-Smith, 2003
Phylum Retaria Cavalier-Smith, 1999
Class Radiolaria Müller, 1859
Subclass Polycystina Ehrenberg, 1839, emend. Riedel, 1967
Order Entactinaria Kozur and Mostler, 1982
Family Quinquecapsulariidae Dumitrica, 1995
Genus _Joergensenium_ Bjørklund, Dumitrica, Dolven and Swanberg, 2008
Type species: _Joergensenium rotatile_ Bjørklund, Dumitrica, Dolven and Swanberg, 2008.

Emended diagnosis: Spherical Quinquecapsulariidae consisting of a double medullary shell (Plate 1, Fig. 2; Plate 2, Figs. 1–3; Plate 5, Fig. 4; Plate 6, Fig. 2) and a single (Plate 1, Fig. 3; Plate 2, Figs. 4–8; Plate 5, Fig. 1; Plate 6, Fig. 1) or a double (Plate 3, Figs. 1–7; Plate 4, Figs. 1–2; Plate 5, Figs. 2–3) cortical shell, both interconnected by more than seven secondary radial bars originating in the second medullary shell and prolonged outside into spines. Microsphere as with the family but

complicated by the appearance of two to four additional bars from the middle of the bars interconnecting the two parallel pentagons and representing lateral edges of the pentagonal prism. Second medullary shell latticed, with a system of arches marked by constrictions that connect the ten radial bars originating in the corner of the pentagonal prism and that repeat at a larger scale the shape of the microsphere.

Discussion: When the genus _Joergensenium_ was described on the basis of its type species (Bjørklund et al., 2008) it seemed difficult to know which of the simple bars interconnecting the two pentagons is the median bar (MB). Based on these new species, that have four curved connecting bars bearing an additional ray originating in their middle, it is easy to recognize the MB in the single bar that has no ray in its middle. In all Mesozoic and Cenozoic evolved entactinarian genera, that are in the genera, that have a more or less complex microsphere with entopically positioned median bar that originated in the four basal rays, the MB is always the simplest bar and the only element that has a triple junction at its ends. On the basis of the present new species, one can easily recognize now the MB of the type species of the genus (Fig. 2.1). It is the bar, surrounded by the two bars that bear two additional rays (ad), and the only bar that lies in the plane of bilateral symmetry of the microsphere. In all the older quinquecapsulariids (the genera _Quinquecapsularia_ Pessagno, _Empirea_ Whalen and Carter) and a new undescribed Paleocene genus with a spherical cortical shell and seven spines originating in the 7 cupolas of the second medullary shell, the bars that interconnect the two pentagons are simple. Therefore, one could suppose that the appearance of additional rays on these bars is an evolutionary character. Moreover, if the number of such rays increases during evolution, one can suppose that _J. arcticum_ n. sp., that has four additional rays, originally developed from _J. rotatile_ that has only two. Unfortunately, this supposition is not yet supported by the range of the two species, which is incompletely known. What we practically know is that the oldest occurrence of _J. rotatile_ is as old as 15,600 calendar years BP (Dolven, 1998; Dolven et al., 2002) and that so far _J. arcticum_ has been found only in the plankton and sinking particle materials in the Chukchi Sea, the western part of the Arctic Ocean.

Table 3
Locations, mooring depths, standard sampling interval, and sample duration of the sediment trap station in the western Arctic Ocean.

Trap station	Latitude	Longitude	Water depth (m)	Mooring depth (m)	Standard sampling interval[a] (days)	Sampled interval
NAP10t	75°00′ N	162°00′W	1975	184 (upper), 1300 (lower)	10–15	4 October 2010–28 September 2011
NAP11t	75°00′ N	162°00′W	1975	260 (upper), 1360 (lower)	10–15	4 October 2011–18 September 2012

[a] Details of the exact durations for each sample are shown in Appendices B and C.

The genus was recorded in both northern and southern oceans during the late Miocene to Quaternary as reported in the recent article by Renaudie and Lazarus (2015). Unfortunately, in spite of the detailed structural work by Dumitrica (in De Wever et al., 2001; and in Bjørklund et al., 2008), Renaudie and Lazarus (loc. cit., text-Fig. 4b) interpreted completely erroneously the structure of the initial spicule and of the first shell (microsphere) of this genus and also of the genus *Lonchosphaera* Popofsky. Neither *Joergensenium* nor *Lonchosphaera* have a single apical ray, as illustrated by them, but a median bar, 2 apical rays and 4 basal rays, plus some special connecting arches (see Dumitrica, 2014). Also, based on an equally erroneous citation by Suzuki and Aita (2011) of the paper by De Wever et al. (2001), they do not recognize the persistence of the entactinarian spicular structures during the whole Mesozoic and Cenozoic, including both genera in the spumellarian family Actinommidae. Moreover, Renaudie and Lazarus (loc. cit.) described in a new species of *Joergensenium*, under the name of *Joergensenium pseudodictyocha* Renaudie and Lazarus, a medullary shell of a species of this genus. All species of this Cenozoic genus are characterized by the presence of a single or double cortical shell. It is only missing in the young ontogenetic stages, which may be more frequent at some levels than the mature specimens, and which are always represented by the double medullary shell. Also, to have a complete description of a species, we have to know the mode of connection between the second medullary shell and the inner cortical one, and the structure of the microsphere. Not one of these characters is clearly visible in their images so that practically the species is indeterminable.

Joergensenium arcticum Ikenoue, Dumitrica and Bjørklund n. sp

Text-Fig. 2.2; Plates 1-6.

Synonyms: 2003 *Actinomma leptoderma leptoderma* — Itaki et al. p. 1517; Plate 1, Fig. 12

Holotype: Plate 2, Fig. 7, Station NAP, NAP11t shallow #25, Stored at the National Museum of Nature and Science, Tokyo with registration number MPC-04118, England Finder coordinates E17/4.

Paratype 1: Plate 1, Fig. 1, Station 32, 100–250 m, Stored at the National Museum of Nature and Science, Tokyo with registration number MPC-04119, England Finder coordinates T30/3.

Paratype 2: Plate 1, Fig. 2, Station 32, 100–250 m, Stored at the National Museum of Nature and Science, Tokyo with registration number MPC-04120, England Finder coordinates J10/3.

Paratype 3: Plate 1, Fig. 3, Station 32, 100–250 m, Stored at the National Museum of Nature and Science, Tokyo with registration number MPC-04121, England Finder coordinates K45/4.

Paratype 4: Plate 3, Fig. 6, Station 56, 250–500 m, Stored at the National Museum of Nature and Science, Tokyo with registration number MPC-04122, England Finder coordinates F11/2.

Description: Shell spherical consisting of one simple or double cortical shell and one double medullary shell consisting of microsphere and second medullary shell. Microsphere looks like a pentagonal prism the corners of which bear one ray. One lateral edge is straight, the other four are curved and bear also a ray in their middle, so that the total number of rays originated in the microsphere is 14. All microspheric rays stop in the wall of the second medullary shell (partly seen on Plate 2, Figs. 1c, 2a, 3c; Plate 6, Figs. 2b–c) and are interconnected by arches that form in its wall with slightly marked constrictions and slightly marked cupolas. Second medullary shell thin-walled with rounded pores of irregular size and arrangement. Their cupolas bear one to two three-bladed radial bars prolonged outside the cortical shell into about 10–15 relatively long pointed spines. Cortical shell is spherical and may be single (Plate 2, Figs. 4–8; Plate 5, Fig. 1; Plate 6, Fig. 1) or double (Plate 3, Figs. 1–7; Plate 4, Figs. 1–2; Plate 5, Figs. 2–3). When single, it is thin walled and has rounded pores of various shapes, sizes and arrangement (Plate 2, Fig. 7a; Plate 5, Fig. 1). When double, the external one is close to the internal shell, spongy-like, fibrillar, formed of thin threads uniting very irregularly the ends of numerous by-spines arising from the wall of the inner cortical shell (Plate 3, Figs. 3, 5–6; Plate 5, Figs. 2–3).

Material: Numerous specimens, juvenile and adult forms with all of the in-between growth stages.

Dimensions: (averaged based on 20 specimens; Table 4): Diameter of microsphere 20 μm (18–24 μm, of second medullary shell 42 μm (39–47 μm, of cortical shell 84 μm (75–94 μm), of second cortical shell 108 μm (96–124 μm).

*Etymology*: From its occurrence in the Arctic Ocean.

Range and occurrence: This species is living mainly in the upper water layers (100–250 m depth) and increase in number during early stage of sea-ice formation (see Chapter 4.2 below). Its first occurrence

Table 4

Diameter measurements of the four shells in *Joergensenium arcticum* n. sp. from the western Arctic Ocean.

Samples	1. shell	2. shell	3. shell	4. shell	Specimen no.	Plate	Collection no.
Sediment trap							
Station NAP, NAP11t, #25	19	45	90	*	Holotype	Plate 2, Figs. 7a–c	MPC-04118
Plankton net							
Station 32 100–250 m	22	44	*	*	Paratype 1	Plate 1, Figs. 1a–d	MPC-04119
Station 32 100–250 m	22	46	*	*	Paratype 2	Plate 1, Fig. 2	MPC-04120
Station 32 100–250 m	20	47	*	*	Paratype 3	Plate 1, Fig. 3	MPC-04121
Station 56 250–500 m	20	40	80	112	Paratype 4	Plate 3, Figs. 6a–c	MPC-04122
Station 32 100–250 m	21	45	*	*		Plate 2, Figs. 1a–c	
Station 56 100–250 m	22	40	*	*		Plate 2, Figs. 2a–b	
Station 56 250–500 m	21	43	*	*		Plate 2, Figs. 3a–c	
Station 56 100–250 m	24	41	83	*		Plate 2, Figs. 4a–b	
Station 56 100–250 m	19	41	85	*		Plate 2, Figs. 5a–b	
Station 32 100–250 m	21	42	75	*		Plate 2, Figs. 6a–c	
Station 32 100–250 m	20	41	94	*		Plate 2, Figs. 8a–c	
Station 56 250–500 m	22	40	88	*		Plate 3, Figs. 1a–b	
Station 56 100–250 m	18	39	76	101		Plate 3, Figs. 2a–b	
Station 32 100–250 m	21	44	89	124		Plate 3, Figs. 3a–c	
Station 32 100–250 m	20	40	79	96		Plate 3, Figs. 4a–c	
Station 56 250–500 m	19	41	81	102		Plate 3, Figs. 5a–c	
Station 56 250–500 m	20	41	86	110		Plate 3, Figs. 7a–b	
Station 56 100–250 m	18	43	86	108		Plate 4, Figs. 1a–b	
Station 56 250–500 m	20	44	83	108		Plate 4, Figs. 2a–b	
Average diameter (μm)	20	42	84	108			

* Means no data.

1a

1b

20 μm

1c

1d

50 μm

2

3
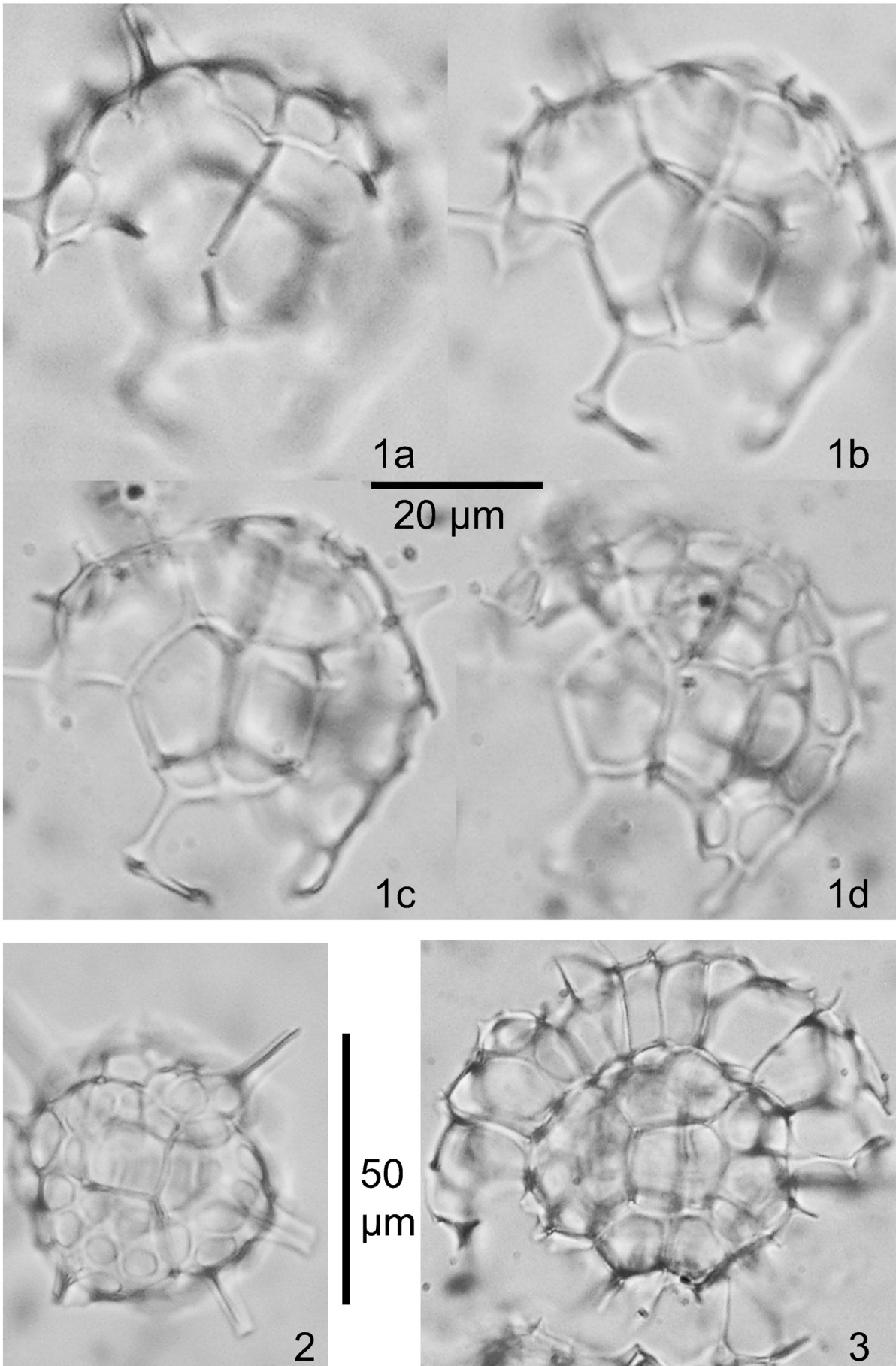
is not known as most cores with Tertiary as well as Quaternary sediments in the Arctic Ocean usually are barren for siliceous microfossils.

Remarks: This species was identified as *Joergensenium* sp. A in Ikenoue et al. (2015), Plate 4, Figs 1–3). Whether this species is being recruited from the Pacific Ocean via the Bering Sea is not confirmed by the plankton data from the south-western part of the shallow Chukchi Sea, presented in this paper. However, the samples studied are essentially barren of any radiolarian fauna, only three species were observed and none of them was *J. arcticum*.

As mentioned under the genus description, structurally, the microsphere consists of an initial spicule formed of a median bar (MB), two apical rays (A), and four basal rays (B). Basal rays are united by a system of arches that form together with MB a pentagonal prism, and each of its ten corners bears a ray. One lateral edge of this prism (MB) is simple, the other four are curved and in their middle they bear an additional radial bar (a), so that the total number of rays extending from the microsphere is 14 (Text-Fig. 2.2). Their distal ends stop in the wall of the outer medullary shell where they are united by arches forming slightly marked constrictions that repeat, by their position, the edges of the macrospheric pentagonal prism. Morphologically, by having 3–4 concentric shells and many radial spines the species *J. arcticum* n. sp. could be considered close to the series of boreal species *Actinomma boreale* (Cleve), *Actinomma leptodermum* (Jørgensen), *Drymyomma elegans* Jørgensen belonging to Actinommidae of Spumellaria (see Bjørklund, 1974a, 1974b, 1976; Cortese and Bjørklund, 1997). These actinommids have a round microsphere with rather small and regular pores. A major difference between *J. arcticum* and the actinommids is the complicated structure of the microsphere in *J. arcticum* that we have mentioned under the species description.

Joergensenium clevei Dumitrica and Bjørklund n. sp

Text-Fig. 2.3; Plate 7.

Description: Test as with the genus, consisting of 3 concentric shells of which one is cortical and two medullary. Cortical shell thin-walled, spherical with numerous polygonal (usually pentagonal or hexagonal) pores arranged irregularly and of relatively equal size (Plate 7, Figs. 1a, 2a). It is covered by numerous small by-spines originating not in the vertices of the pore frames but on the intervening bars of the frames (Plate 7, Fig. 1). Sometimes, and on some portions, they can be interconnected by very thin bars. Microsphere has a shape of a short pentagonal prism with one lateral edge simple and straight or slightly curved, representing the MB, and the other four curved and provided with an additional radial bar (ad) in their middle. All corners represent points of origin of 10 rays, of which 2, at the ends of MB, are apical (A), 4 are basal (B), and the other 4 are antapical (ant), refer to Text-Fig. 2.3. At the level of the second medullary shell, all these rays are interconnected by arches forming a second prismatic shell with curved edges that repeats the fundamental shape of the microsphere. Second medullary shell has 7 cupolas erected on these edges (some cupolas are seen in Plate 7, Figs. 1b, 2c–e) and corresponding to the 7 facets of the polygonal prism. Cupolas are well marked especially in axial view, which is the view along the MB. All the 14 rays originate in the microsphere periphery in the arches of the second medullary shell, and only occasionally1–2 rays may be prolonged as thin rays up to the cortical shell. The tops of the 7 cupolas are at the origin of 7, three-bladed radial bars that traverse the cortical shell and extend outside it into pointed spines that usually are not longer than their inner portion.

Material: Two specimens observed in Cleve's slide collection, located on Cleve slide #33.

Holotype: Plate 7, Fig. 2. Stored at the Swedish Museum for Natural History with registration number SMNH Type-6120-1, England Finder coordinates J40/1.

Paratype: Plate 7, Fig. 1. Stored at the Swedish Museum for Natural History with registration number SMNH Type-6120-2, England Finder coordinates G36/0.

Dimensions: Holotype: Diameter of microsphere 25 μm, of second medullary shell 46 μm, of cortical shell 101 μm. Paratype: Diameter of microsphere 27 μm, of second medullary shell 50 μm, of cortical shell 110 μm.

Etymology: The species is dedicated to the Swedish chemist, biologist, mineralogist, oceanographer Per Teodor Cleve (1840–1905) for his contribution to the knowledge of the radiolarians from the Spitzbergen area.

Range: So far this species has only been found in plankton material east of Spitzbergen (78° 18′N, 2° 58′W). An additional observation of *J. clevei* was made in DSDP Site 609, 2CC in the North Atlantic with an estimated age of about 313,000 years (Ciesielski and Bjørklund, 1995). The stratigraphic occurrence of this species was not looked for either below or above the 2CC sample. The stratigraphic significance of this species is therefore not known at present.

Remarks: *Joergensenium clevei* Dumitrica and Bjørklund n. sp. resembles *J. arcticum* Ikenoue, Dumitrica and Bjørklund n. sp., from which it differs in being much more regular, in having practically only 7 external spines, and in having the cortical shell normally one-shelled. It is possible that they are 2 contemporaneous species characterizing 2 geographical areas, the former the north Atlantic and the latter the north-western part of the Arctic Ocean with its main distribution and abundance in the Chukchi Sea. According to Cleve's slide #33 the sampling was from 2000 m to the surface. In Cleve's several slides, covering the sampling depth shallower than ca 400 m, no *J. clevei* was observed. *Joergensenium rotatilis* is observed in west Norwegian fjord plankton and is endemic to rather warm water (7 °C). *Joergensenium rotatilis* is also found in surface sediment samples in the Norwegian Sea, but we have so far no information on which water mass it belongs to. As we have not observed *J. clevei* in our west Norwegian fjord fauna we assume this species might be a deep (>400 m) and cold water dweller, originating from the Arctic Ocean, and occupying the water masses underlying the warm Norwegian Sea Current (the continuation of the North Atlantic Current) in the area west of Spitzbergen. In conclusion, we may suggest the following: *J. rotatile* is a warm water boreal species with its home area in the Nordic Seas and the Norwegian fjords, *J. clevei* with a subarctic distribution in the northern part of the Norwegian Sea, and finally *J. arcticum* in the western part of the Arctic Ocean, probably endemic to the Chukchi Sea area, as it has not been registered elsewhere so far.

4.2. Vertical distribution and flux variation of Joergensenium arcticum in the northern Chukchi Sea

The vertical distribution of *J. arcticum* at five stations in the northern Chukchi Sea are shown with hydrographic profiles (Nishino, 2013) in Fig. 3. *Joergensenium arcticum* was absent at 0–100 m depth, but abundant at 100–250 m depth, and rare at deeper depths at stations 32 and 56. The standing stocks of *J. arcticum* at 0–150 m depth at stations 31 (same coordinates as Station 32) and 56 were somewhat lower than that at 100–250 m depth at stations 32 and 56, respectively, but the ratio of juvenile forms of *J. arcticum* was higher. The highest standing stock of *J. arcticum* was observed at Station 54 at 0–150 m depth, while
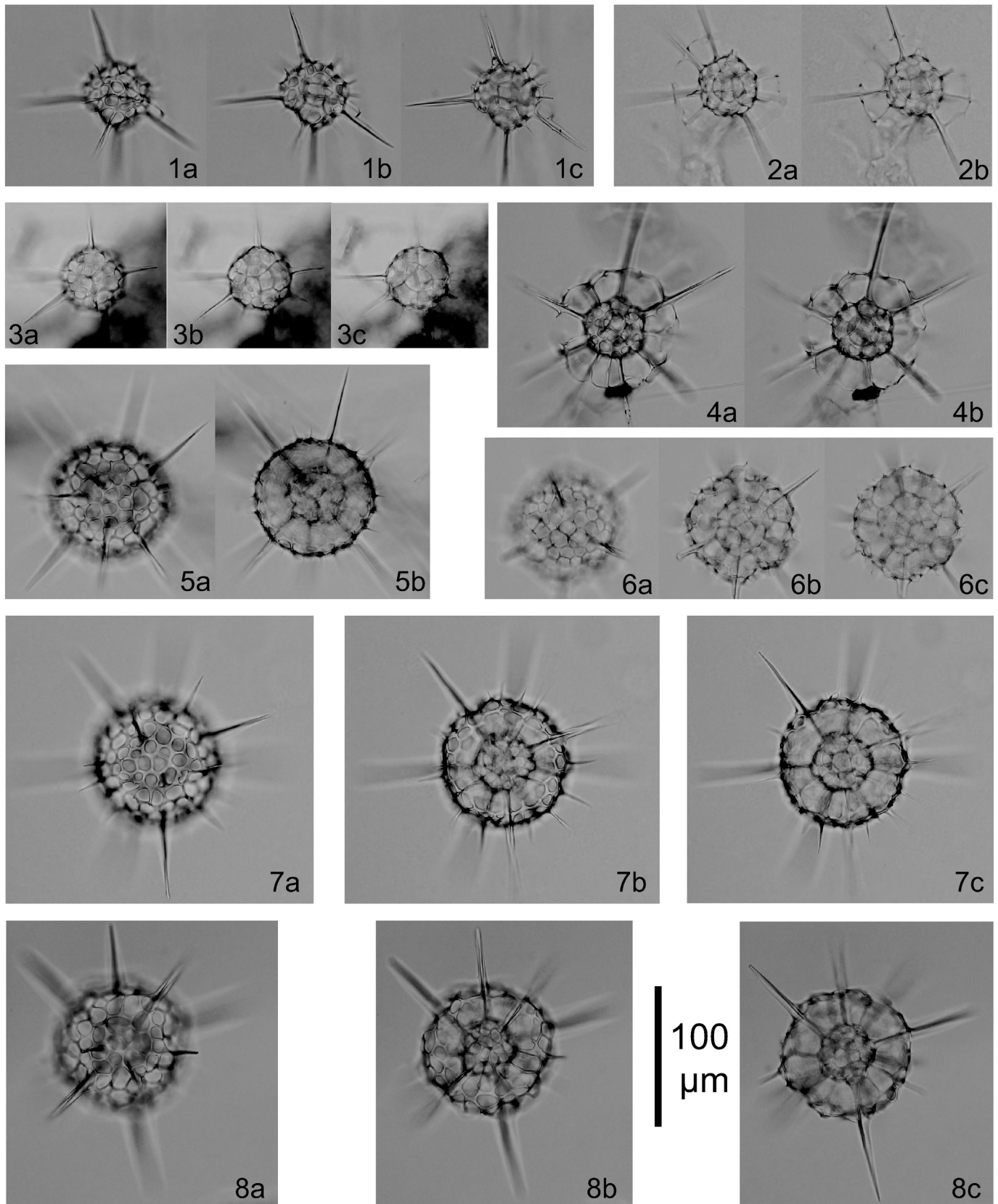
Plate 1. Transmitted light micrographs of 3 specimens of *Joergensenium arcticum* Ikenoue, Dumitrica and Bjørklund n. sp. showing the microsphere, the second medullary shell (Figs. 1–2) and the entire specimen (Fig. 3). 1a–d — broken specimen of which the microsphere was drawn in text-Fig. 2, focused at 4 levels. 2 — Medullary shell of a specimen focused under the surface showing inside the microsphere. 3 — Entire specimen focused at the equatorial plane with the microsphere in lateral view. Scale bar = 20 μm for Fig. 1. Scale bar = 50 μm for Figs. 2–3.Plate 1
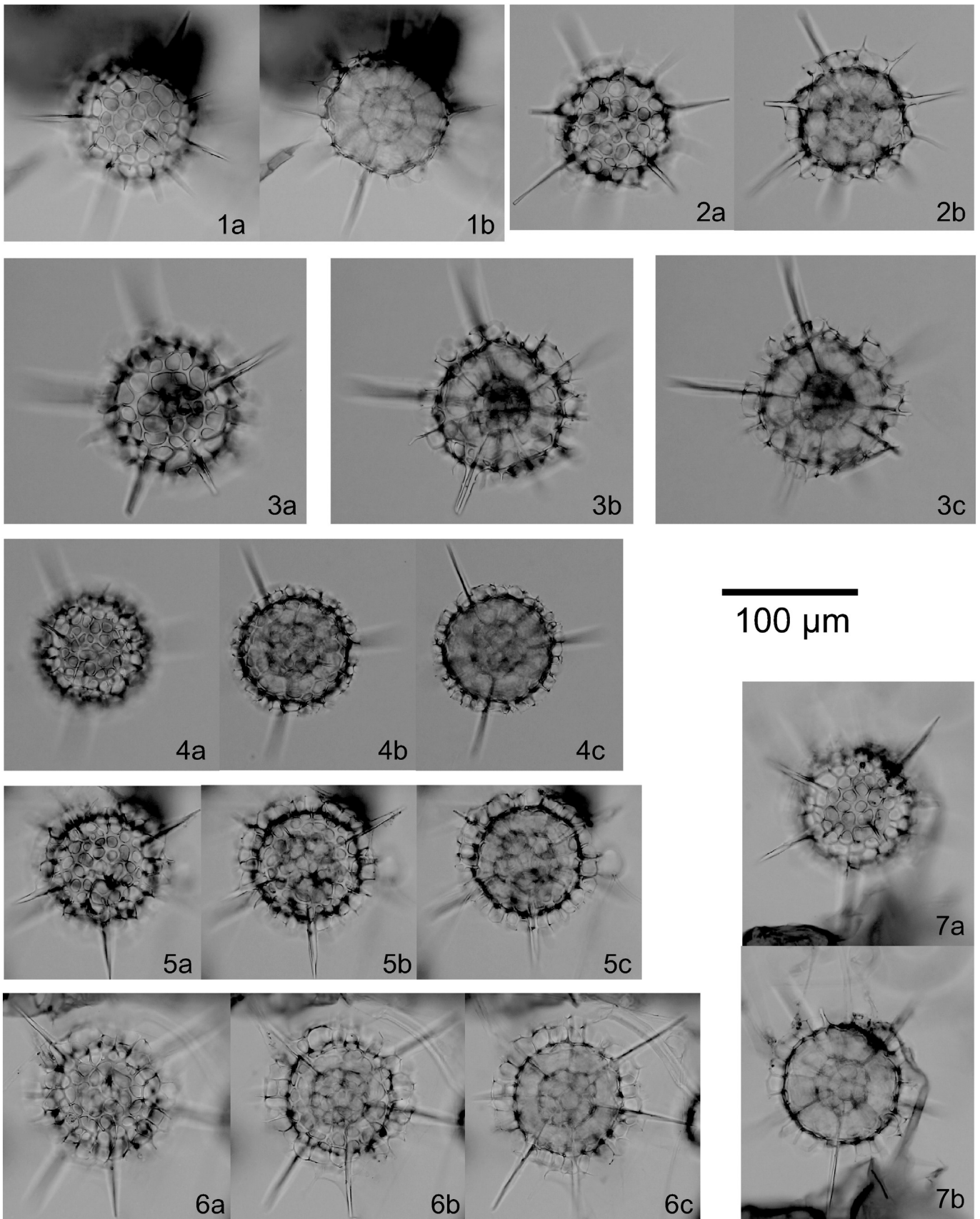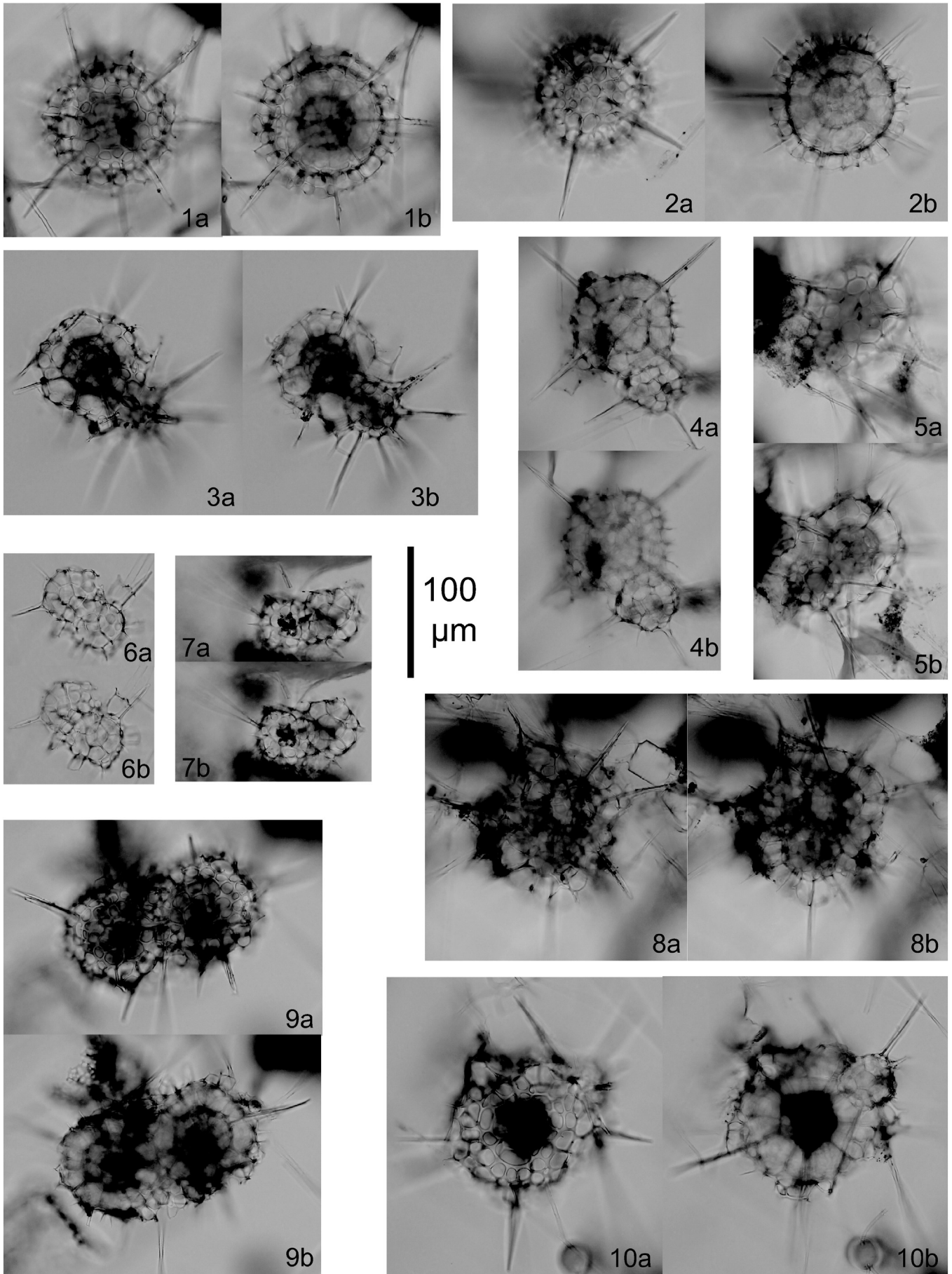
Plate 2. Transmitted light micrographs of *Joergensenium arcticum* Ikenoue, Dumitrica and Bjørklund n. sp. (Figs. 1–8). 1a–c. *Joergensenium arcticum* juvenile form, same specimen. Station 32, 100–250 m. 2a–b. *Joergensenium arcticum* juvenile form, same specimen. Station 56, 100–250 m. 3a–c. *Joergensenium arcticum* juvenile form, same specimen. Station 56, 250–500 m. 4a–b. *Joergensenium arcticum*, same specimen. Station 56, 100–250 m. 5a–b. *Joergensenium arcticum*, same specimen. Station 56, 100–250 m. 6a–c. *Joergensenium arcticum*, same specimen. Station 32, 100–250 m. 7a–c. *Joergensenium arcticum*, same specimen. Station NAP, NAP11t, shallow #25. 8a–c. *Joergensenium arcticum*, same specimen. Station 32, 100–250 m. Scale bar = 100 μm for all figures.

Plate 3. Transmitted light micrographs of *Joergensenium arcticum* Ikenoue, Dumitrica and Bjørklund n. sp. (Figs. 1–7). 1a–b. *Joergensenium arcticum*, same specimen. Station 56, 250–500 m. 2a–b. *Joergensenium arcticum*, same specimen. Station 56, 100–250 m. 3a–c. *Joergensenium arcticum*, same specimen. Station 32, 100–250 m. 4a–c. *Joergensenium arcticum*, same specimen. Station 32, 100–250 m. 5a–c. *Joergensenium arcticum*, same specimen. Station 56, 250–500 m. 6a–c. *Joergensenium arcticum*, same specimen. Station 56, 250–500 m. 7a–b. *Joergensenium arcticum*, same specimen. Station 56, 250–500 m. Scale bar = 100 μm for all figures.

100 μm
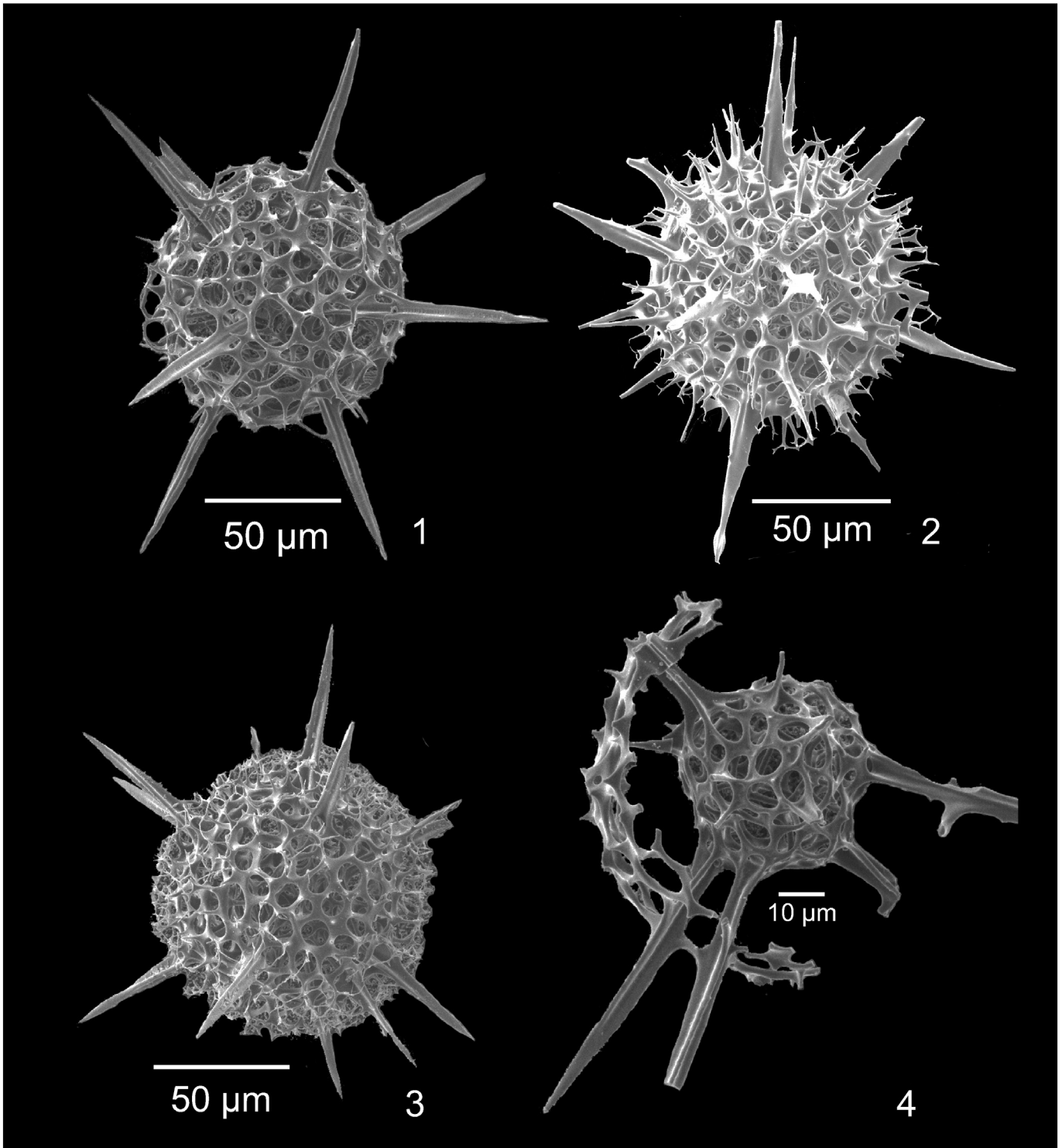
Plate 5. Scanning electron micrographs of *Joergensenium arcticum* Ikenoue, Dumitrica and Bjørklund n. sp. showing the surface general view of cortical and medullary shells (Figs. 1–4). 1. Split specimen showing single cortical shell. Station 32 100–250 m. 2. Split specimen showing early developed second cortical shell. Station 32 100–250 m. 3. Split specimen showing second cortical shell. Station 32 100–250 m. 4. Split specimen showing second medullary shell with broken cortical shell. Station 32 100–250 m. Scale bar = 50 μm for Figs. 1–3. Scale bar = 10 μm for Fig. 4.

Plate 4. Transmitted light micrographs of *Joergensenium arcticum* Ikenoue, Dumitrica and Bjørklund n. sp. (Figs. 1–2). 1a–b. *Joergensenium arcticum*, same specimen. Station 56, 100–250 m. 2a–b. *Joergensenium arcticum*, same specimen. Station 56, 250–500 m. Transmitted light micrographs of conjoined *Joergensenium arcticum* skeletons (Figs. 3–10). 3a–b. 2nd–2nd order of conjoinment, same specimen. Station 32, 100–250 m. 4a–b. 2nd–3rd order of conjoinment, same specimen. Station 56, 250–500 m. 5a–b. 2nd–2nd order of conjoinment, same specimen. Station 56, 100–250 m. 6a–b. 1st–2nd order of conjoinment, same specimen. Station 56, 500–1000 m. 7a–b. 1st–2nd order of conjoinment, same specimen. Station 32, 100–250 m. 8a–b. 2nd–2nd–2nd order of conjoinment, same specimen. Station 56, 100–250 m. 9a–b. 3rd–3rd order of conjoinment, same specimen. Station 56, 100–250 m. 10a–b. 2nd–3rd order of conjoinment, same specimen. Station 56, 100–250 m. Scale bar = 100 μm for all figures.
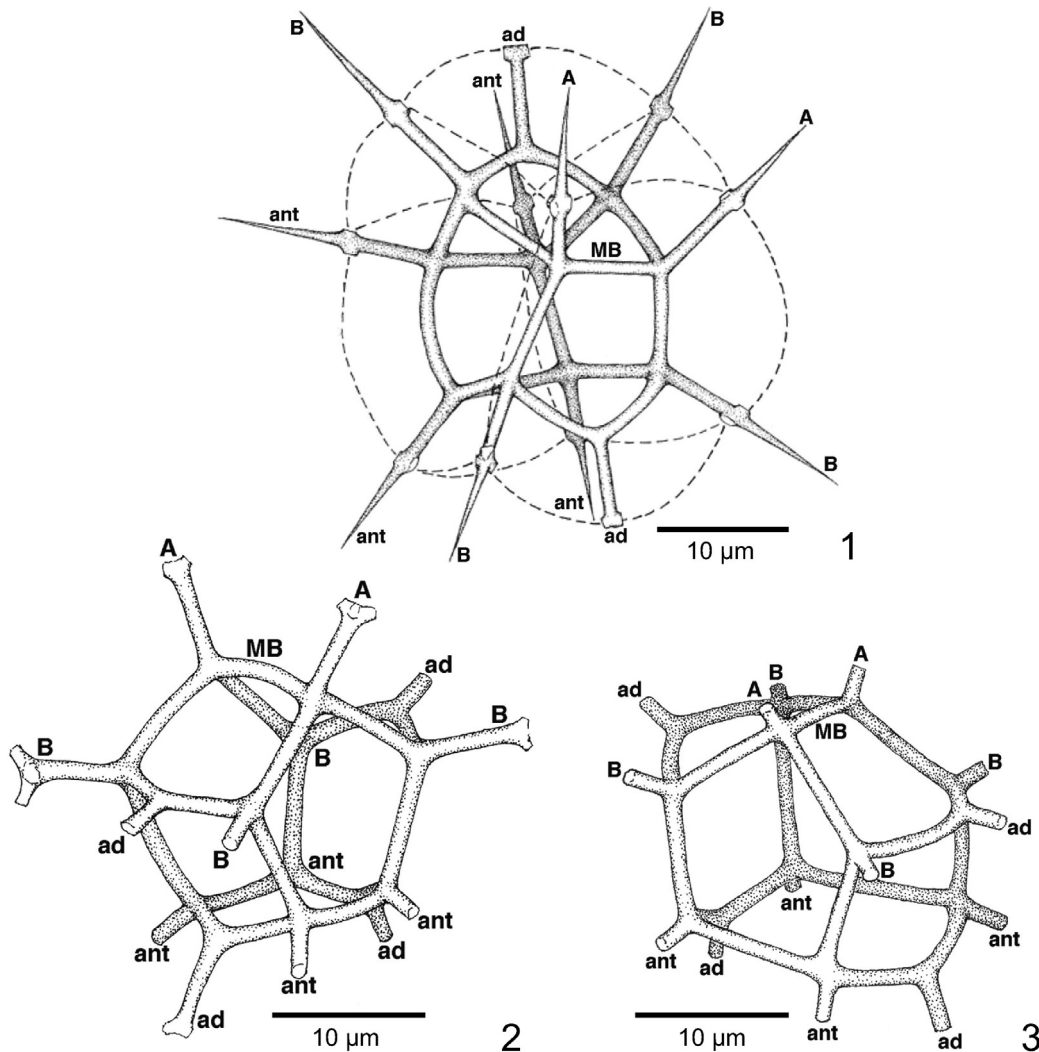
Fig. 2. Comparative structure of the microsphere of the species *Joergensenium rotatile*, *Joergensenium arcticum* n. sp., and *Joergensenium clevei* n. sp. 1 — *Joergensenium rotatile* Bjørklund, Dumitrica, Dolven and Swanberg, slightly oblique apical view. 2 — *Joergensenium arcticum* n. sp., oblique lateral view. 3 — *Joergensenium clevei* n. sp., oblique lateral view. MB — median bar, A — apical rays, B — basal rays, ant — antapical rays, ad — additional rays. Dotted line in Fig. 1 marks the position of the arch on the second medullary shell. The same arches are also present in the wall of *J. arcticum* and *J. clevei*. Scale bars = 10 μm.

J. arcticum was absent at Station 52 at 0–66 m depth. We also observed a few specimens of conjoined skeletons of *J. arcticum* (Table 1; Plate 4, Figs. 3–10) and they were found mainly in the PWW layer at stations 32 and 56.

The flux of *J. arcticum* increased during the early stage of sea-ice formation in the upper and lower traps except for summer in 2012 (Fig. 4). Juvenile form of *J. arcticum* occurred mainly during the sea-ice-cover season. The counted numbers of *J. arcticum* are shown in Appendices B and C.

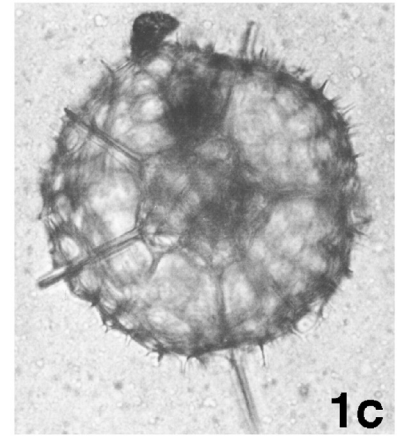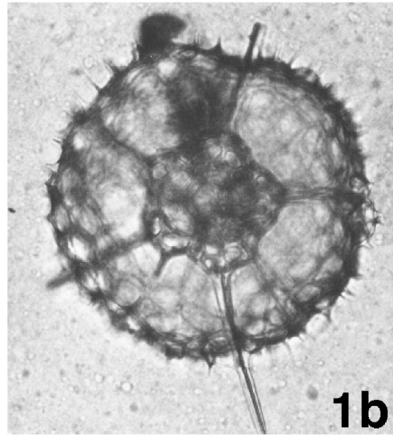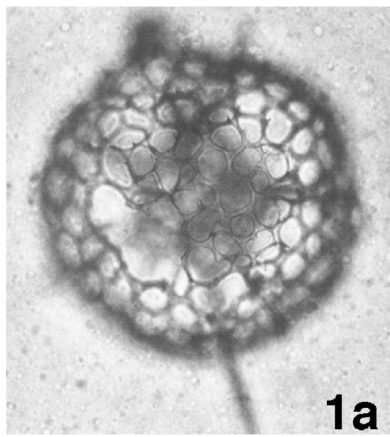### 4.3. Radiolarian standing stocks in the Bering Strait and southern Chukchi Sea

The radiolarian standing stocks in the Bering Strait and southern Chukchi Sea are shown in Table 2. Radiolarians were not found at stations 1, 3, 5, 7, 8, and 9 at all, indicating that the standing stock is zero at the time when our samples were collected in the open part of the southern Chukchi Sea. However, only a few fragments of radiolarian skeletons were found at two stations located closest to the shore, stations 68 and 70 (Fig. 1). One juvenile spumellarian species (*Actinomma*? sp. juvenile) and one juvenile nassellarian species (*Ceratospyris borealis*? juvenile) were found at Station 68 (Fig. 5.1 and 5.2a–b, respectively), while only one spumellarian species (*Stylodictya* sp.) was found at Station 70 (Fig. 5.3a–b). The standing stocks for these two stations are six (Station 68) and two (Station 70). These values are again close to zero which supports the other plankton data from the more open part of the southern Chukchi Sea, documenting an almost non-existing introduction of Pacific forms during the period of sampling.
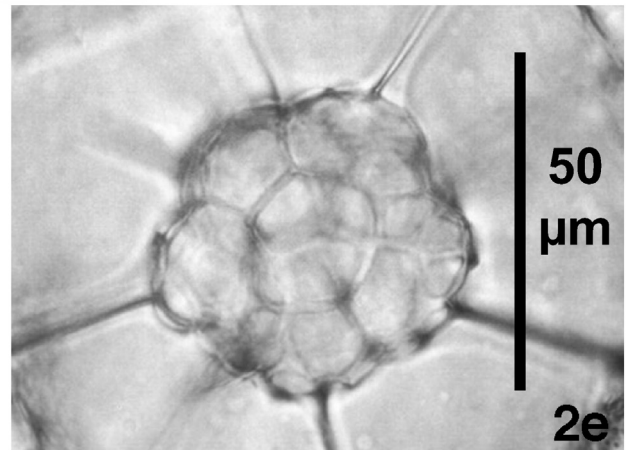
4.4. Symbionts of Joergensenium arcticum

Polymerase chain reaction on SCWGA material from 10 radiolarian cells yielded 10 MALV (Marine alveolate) partial 18S rDNA sequences (Table 5). Sequences from eight individuals of *J. arcticum* grouped within the MALV Group I; of these eight four grouped within the already
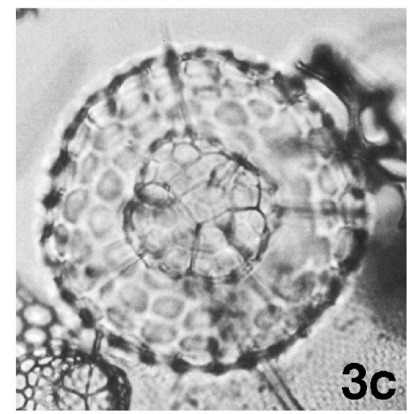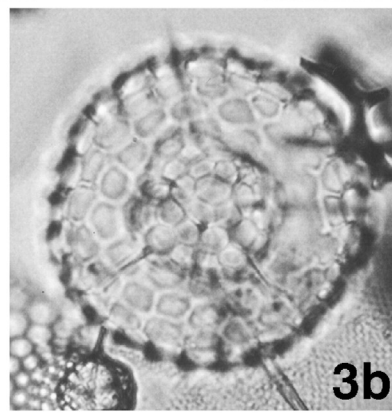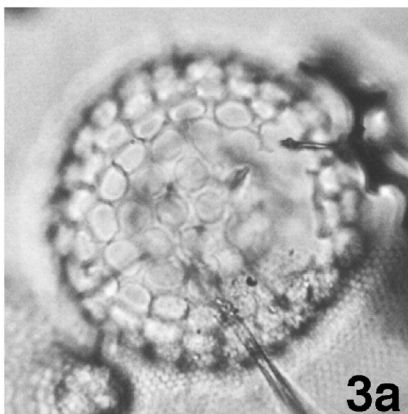
Plate 6. Microfocus X-ray Computed Tomography cross-sectional images of *Joergensenium arcticum* Ikenoue, Dumitrica and Bjørklund n. sp. showing taxonomic characters of this species (Figs. 1–3). 1–3. *Joergensenium arcticum*, same specimen, Station 54, 0–150 m. 1a–d. A series of xy cross sectional image of general over view. Scale bar = 50 μm for all Figs. 2a–c. A series of xy cross sectional images of a second medullary shell. Scale bar = 10 μm for all Figs. 3. Segmented image of a microsphere, oblique lateral view. Scale bar = 10 μm. MB — median bar, A — apical rays, B — basal rays, ant — antapical rays, ad — additional rays.
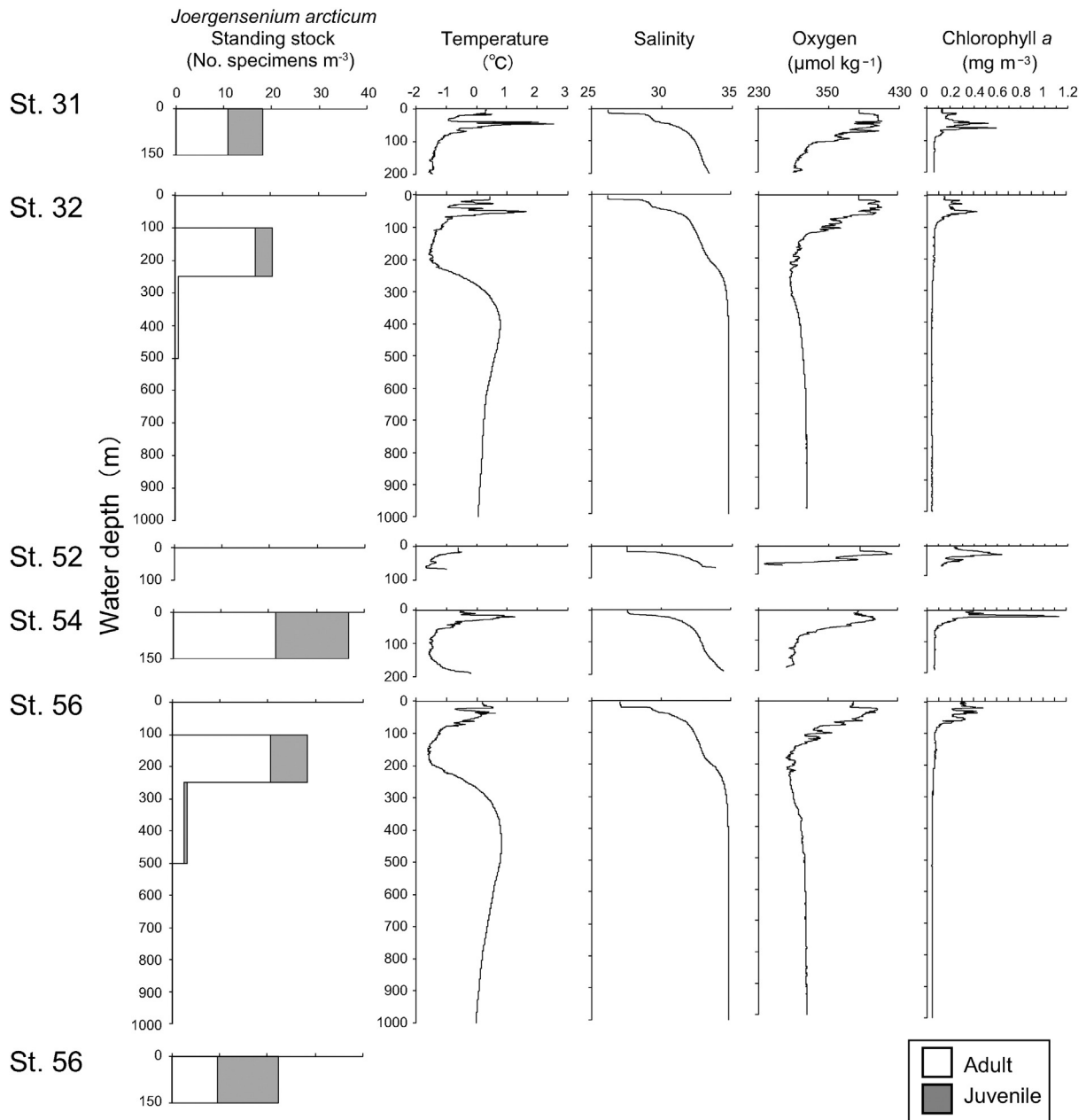
100 μm

50 μm

Fig. 3. Depth distributions of *Joergensenium arcticum* in the northern Chukchi Sea in comparison to vertical profiles of temperature, salinity, dissolved oxygen, and chlorophyll *a* (Nishino, 2013).

established RAS 1 (Radiolarian associated sequences) and one in RHIZ 1 (Rhizarian associated sequences) (terminology from Bråte et al., 2012), while three of the sequences define a new subclade (RAS 6), distantly related to RAS 2 (Fig. 6). Two sequences are placed in the MALV Group II, defining a new clade called RAS 5, distantly related to RAS 4.

5. Discussion

Joergensenium arcticum was absent in the SML and PSW (0–100 m depth) and was abundant in the PWW (100–250 m depth) at stations 32 and 56 (Fig. 3). However, in the 150–0 m vertical tows at stations 31 (same coordinates as for station 32), 54, and 56, *J. arcticum* was fairly

abundant, and the ratios of their juvenile forms were higher than in the 250–100 m vertical tows at station 32 and 56 (Fig. 3). Therefore, a substantial part of the *J. arcticum* population should be concentrated within the 100–150 m depth zone and the juvenile forms might relatively be more common in the upper part of the 100–250 m depth zone. According to our hydrographical data from the different stations, *J. arcticum* should prefer colder (< -1.2 °C) and saltier (at least > 32) water masses than what is characteristic for SML and PSW. The highest standing stock of *J. arcticum* was observed at 0–150 m depth at Station 54 where the depth of minimum temperature (126 m depth) was shallower than at the other stations (194 m at Station 31; 182 m at Station 32; 151 m at Station 56) (Fig. 3). This is probably because the PWW, which

Plate 7. Transmitted light micrographs of *Joergensenium clevei* Dumitrica and Bjørklund n. sp. (Figs. 1–3). 1a–c. *Joergensenium clevei*, same specimen focused at 3 levels. Cleve slide #33. 2a–d. *Joergensenium clevei*, same specimen focused at four levels; 2e. same specimen, detail of medullary shell. Cleve slide #33. 3a–c. *Joergensenium clevei*, same specimen focused at 3 levels. DSDP-609, 2CC. Scale bar = 100 µm for all figures except for 2e whose scale bar is 50 µm.
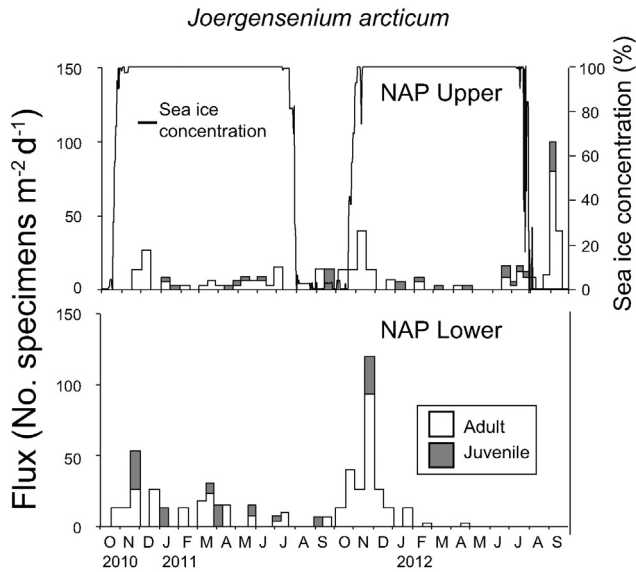
Fig. 4. Two-year fluxes of *Joergensenium arcticum* at Station NAP during the sampling period.

J. arcticum prefers, mostly fell within the range of 100–150 m at Station 54. No *J. arcticum* and no other radiolarians were found at the shallow (71 m) Station 52 (Fig. 3), although the temperature and salinity at 39–66 m depth does satisfy the preferred living conditions of *J. arcticum*. *Joergensenium arcticum* is not present in any of the plankton material north of the Bering Strait that we have investigated from depths shallower than about 70 m.

Conjoined skeletons of *J. arcticum* were mainly found in the PWW layer (Table 1). Itaki and Bjørklund (2007) reported 104 specimens of conjoined actinommid skeletons from the Sea of Japan. They suggested that the very cold temperature may possibly inhibit full separation of cytoplasmically joined individuals, and was interpreted as evidence for asexual reproduction. We have observed conjoined skeletons of the orders 1st–2nd (junction of first and second shell), 2nd–2nd (junction of second and second shell), 2nd–3rd and 3rd–3rd (see Itaki and Bjørklund (2007) for details) verifying that skeletons of classical one and two shelled juvenile forms and three or more shelled adult specimens are joined. We do not see how this can come into existence through a sexual reproduction line as we then would have an individual development of both the soft tissue and the solid skeleton part of the specimen. The data of Itaki and Bjørklund, from two cores in the Japan Sea, showed that the abundance of conjoined skeletons increased with periods in the late Holocene (5 ka) and late Pleistocene (13 ka) when opal production was much higher in the surface waters (Lee et al., 2003) and when the Japan Sea bottom water was well oxygenated (Tada et al., 1999). Itaki and Bjørklund (2007) therefore concluded that an increase in conjoined skeletons could be associated with cold deep-water that was characterized by high oxygen content and rich in nutrients. Our data also indicate that conjoined skeletons occur in very cold-water mass and high oxygen conditions. However, in the Arctic Ocean conjoined skeletons is a shallow water phenomenon.

Joergensenium arcticum lives in the PWW and its flux variation might be related to changes within this water mass during the sampling period. The flux of *J. arcticum* increased during the early stage of sea-ice formation during October–November both in 2011 and 2012 (Fig. 4). Its peak occurrence might indicate a supply and mixing of a cold and more saline water mass with the PWW by brine drainage (Melling and Lewis, 1982; Aagaard et al., 1985). During the sea-ice-cover season when food supply is limited in the water column, *J. arcticum* might survive as juvenile forms. During May–September 2012, most of the radiolarian flux at the lower trap was extremely low and probably due to a decrease in aggregate formation by influx of oligotrophic surface
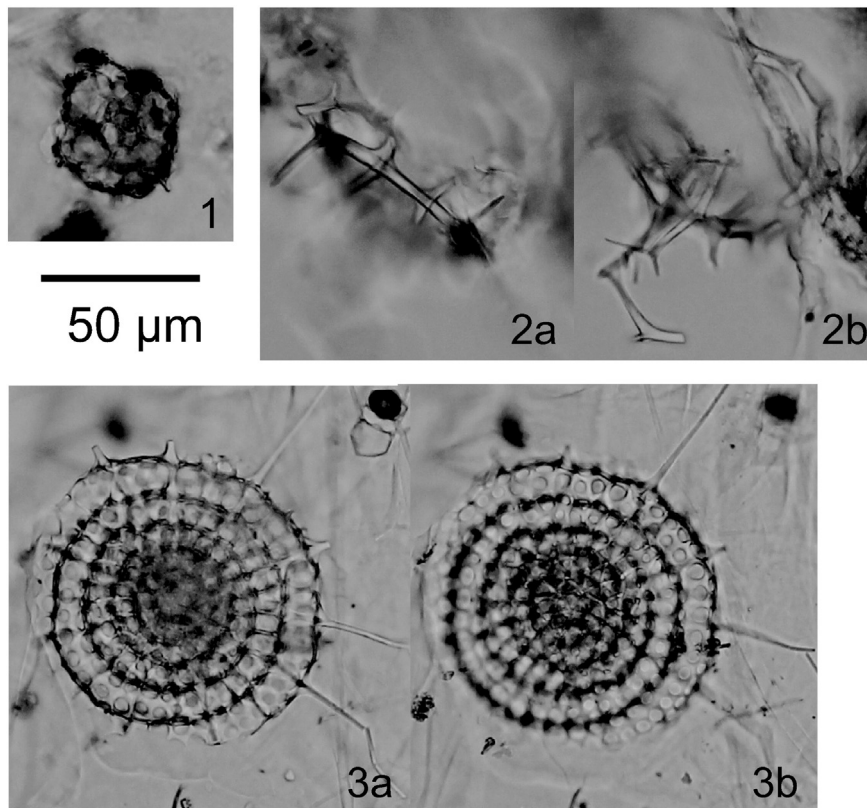

Fig. 5. Radiolarian skeletons in the Bering Strait and southern Chukchi Sea. 1. *Actinomma*? sp. juvenile, station 68. 2a–b. *Ceratocyrtis borealis*? juvenile, same specimen, station 68. 3a–b. *Stylodictya* sp., same specimen, station 70. Scale bar = 50 μm for all figures.
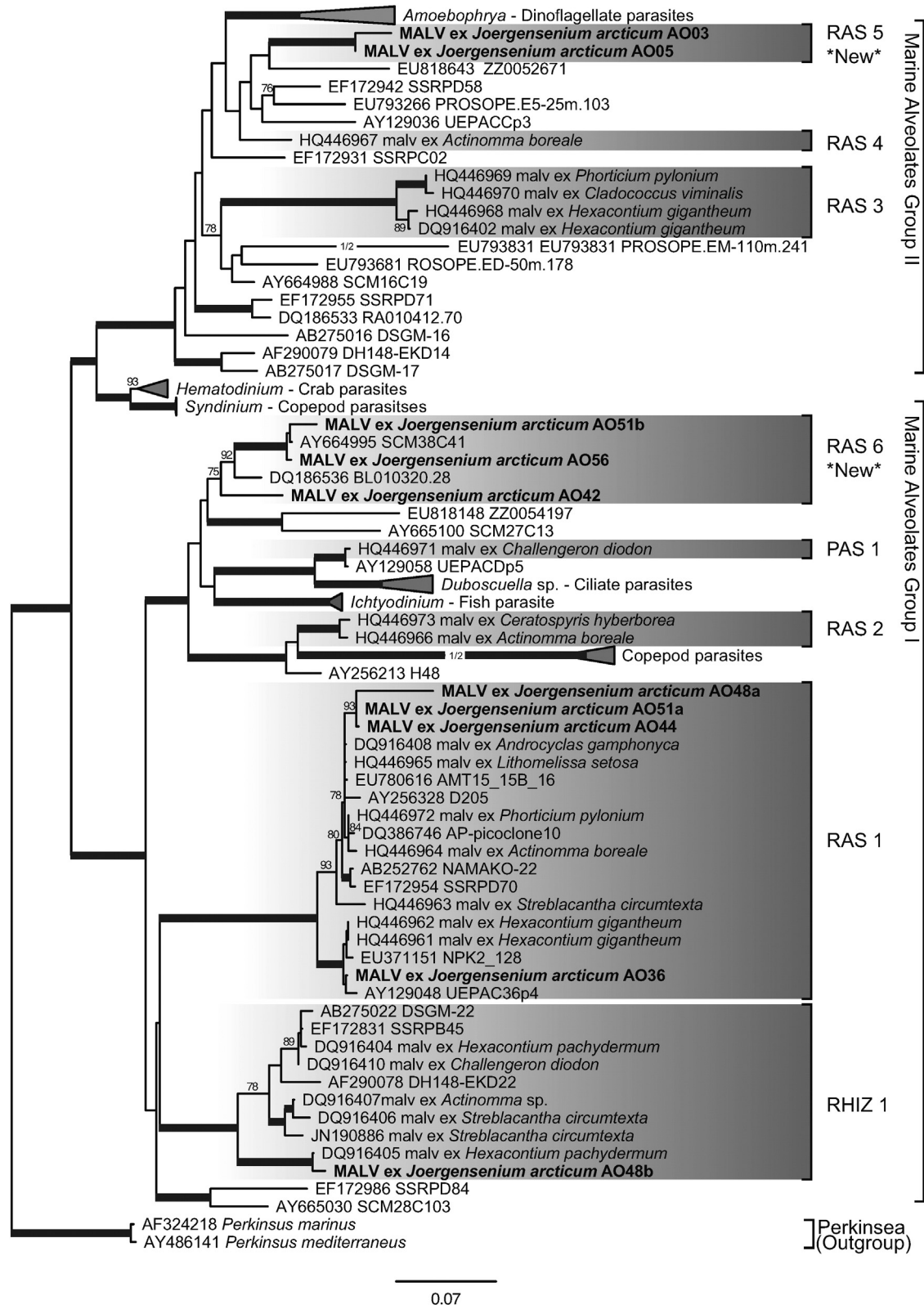
Fig. 6. 18S rDNA phylogeny of marine alveolates group I and group II inferred by maximum likelihood analysis. Gray shaded boxes indicate clades containing marine alveolates associated with radiolarian and rhizarian species. RAS 1–6 = Radiolarian associated sequences clades 1–6, RHIZ 1 = Rhizarian associated sequences, PAS 1 = Phaeodarian associated sequences. Sequences generated in this study are shown in bold. Thick branches have a bootstrap support of 100%; values below 75% are not shown. Because of space limitations some branches are shortened to half their length (marked with 1/2) and some clades are collapsed.

water originating from the Beaufort Gyre in the Canada Basin (Ikenoue et al., 2015). The flux values of *J. arcticum* in the lower trap were also extremely low (Fig. 4) and was not exported to the deep sea during May–

September 2012, while that in the upper trap showed the highest peak in September 2012. We propose that oligotrophic water suppressed the flux of *J. arcticum* until August 2012. Furthermore, at the end of the sea-

Table 5
List of symbiont sequences from *Joergensenium arcticum* used for the phylogenetic analysis in this study.

Host sample name	Host Species	Station	MDA	Symbiont	Associated group
AO03	*J. arcticum*	56	5/21/2014	Marine alveolate	RAS 5
AO05	*J. arcticum*	54	5/21/2014	Marine alveolate	RAS 5
AO36	*J. arcticum*	31	5/21/2014	Marine alveolate	RAS 1
AO42	*J. arcticum*	54	11/30/2014	Marine alveolate	RAS 6
AO44	*J. arcticum*	54	11/30/2014	Marine alveolate	RAS 1
AO48a	*J. arcticum*	54	11/30/2014	Marine alveolate	RAS 1
AO48b	*J. arcticum*	54	11/30/2014	Marine alveolate	RHIZ 1
AO51a	*J. arcticum*	54	11/30/2014	Marine alveolate	RAS 1
AO51b	*J. arcticum*	54	11/30/2014	Marine alveolate	RAS 6
AO56	*J. arcticum*	54	11/30/2014	Marine alveolate	RAS 6

ice-cover season, the conditions might result in a remaining cold water mass and an increase in food availability, and therefore an associated increase in the *J. arcticum* flux in the upper trap.

In the Bering Strait and southern Chukchi Sea, *J. arcticum* was not found in our plankton samples, and other radiolarians were similarly scarce or absent (Table 2). Sediment data from the shallow northern part of the Bering Sea (Blueford, 1983) and southern part of the Chukchi Sea are barren of radiolarian skeletons, and therefore we could not document if there is a present day active migration of radiolarians from the Pacific realm into the Arctic province. There is so far, to our knowledge, no written documentation of plankton tow information from this area proving the occurrence of such an active migration. We herein for the first time, based on plankton tows from six stations (St. 1–St. 9) from the Bering Strait passage to about 68°30′ N, document that there is no significant invasion of radiolarians from the Bering Sea to the western Arctic Ocean (Fig. 1). Only traces at two stations (St. 68 and St. 79) of three species (*Actinomma*? sp. juvenile, *Ceratospyris borealis*? juvenile, and *Stylodictya* sp.) have been observed (Fig. 5). *Ceratospyris borealis* is an abundant species in both plankton and sediment in the southwestern deep part of the Bering Sea and *Stylodictya* spp. are also common taxa in the Bering Sea plankton (Ikenoue et al., 2012a). Most likely these specimens have been transported from the Bering Sea by the Alaskan coastal water, but in an insignificant number. Itaki et al. (2003); Bjørklund and Kruglikova (2003) and Ikenoue et al. (2015) suggested that there is little or no transport of radiolarian fauna elements from the Pacific into the Chukchi Sea, a conclusion that is confirmed by the data presented herein. Furthermore, nor have we, or any other researchers, been able to document any established populations of typical Pacific fauna elements in the Chukchi Sea or elsewhere in the Arctic Ocean. In practical terms, during the period of plankton sampling, there is no significant radiolarian migration between the two oceans. This is probably because an active invasion of radiolarians has been prevented by the low salinity water mass and shallow water depth in the Bering Strait and southern Chukchi Sea. The salinity of southern Chukchi Sea is below 32 in winter and below 30 in summer (EWG, 1998). Only one brackish (salinity < 30) radiolarian species (*Lophophaena rioplatensis*) has been recorded in Boltovskoy et al. (2003) from Río de la Plata estuary, but radiolarians are generally very scarce or absent in coastal waters, where salinity falls below normal open-ocean values (Kling, 1978; Anderson, 1983; Caron and Swanberg, 1990; Anderson et al., 2002). Petrushevskaya (1971) listed the salinity ranges of 145 polycystine species in the world ocean, and the lowest value given was 32 (for *Amphimelissa setosa*). The origin and first occurrence of *J. arcticum* in the Arctic Ocean are still unknown, and *J. arcticum* has so far only been observed in plankton and sediment material in the present study era of the Arctic Ocean. We therefore define *J. arcticum* as endemic to the Arctic Ocean and it might serve as an indicator for the PWW layer.

Marine alveolate species are abundant and make up a large portion of the diversity of environmental studies from all major oceans (Not et al., 2007; Guillou et al., 2008; de Vargas et al., 2015). Although the ecological role of this enigmatic group is still largely unknown, much of the evidence gathered suggests that they are at least to a large extent parasitic. All the known groups are parasitic on diverse hosts such as fish, copepods, crabs and other protists (Skovgaard, 2014). It has recently been shown that many radiolarians in Sogndalsfjorden in Norway are associated with marine alveolates (Dolven et al., 2007; Bråte et al., 2012). Several of the sequences obtained from *J. arcticum* in this study follow the same pattern as those in the Norwegian fjords, and fall into the same clades (Fig. 6). Four sequences fall within RAS 1, which already contains representatives from both spumellarian (e.g. *Actinomma boreale*) and nassellarian (e.g. *Lithomelissa setosa*) species, while one sequence groups with a marine alveolate originating from an individual of *Hexacontium pachydermum*, in RHIZ 1. However, the alvoelates from the Arctic Ocean also form two new clades, one in MALV I (called RAS 6, following the naming scheme of Bråte et al., 2012), and another in MALV II (RAS 5). These are most likely new parasitic alveolates. Since the newly obtained MALV sequences are from a different geographical region than those described in Dolven et al. (2007) and Bråte et al. (2012) it increases the probability that the marine alveolates are specifically associated with radiolarian species, and an important factor in the global ecosystem.

Our preliminary results for the MALV species are of special interest because the question about the origin of the MALV species is still unsolved; i.e., from where, how and when they became associated with the radiolarian host cells? Conjoined skeletogenesis was interpreted as a result of asexual reproduction by binary fission. If asexual reproduction is the only mode of reproduction within *J. arcticum*, it is to be expected that the mother and daughter cell both equally divide the cell material as well as the MALV species. This will in turn give a *J. arcticum* population with an almost monospecific MALV population. Our results show evidence that the *J. arcticum* population in the Chukchi Sea does not hold a monospecific MALV population, but that different *J. arcticum* hosts are found in association with different MALV species. Usually we have only one MALV species per host, but we have some examples where two MALV species are found in the same host. Our data suggest that *J. arcticum* probably also has a sexual reproduction stage as different hosts have different MALV species. During sexual reproduction nothing else than the radiolarian genetic material, and thin cytoplasm layer surrounding the DNA-containing nucleus of the presumptive gametes, is involved and shared between the offspring and therefore they are free of any symbionts or parasites. The MALV species must therefore be introduced at a later stage and must be living freely in the water column and may be incorporated in the host cell when they make contact in the water column.

6. Conclusion

We have described two new living Entactinaria species from the Arctic province: *J. arcticum* and *J. clevei*. *Joergensenium arcticum* is probably endemic to the Arctic Ocean and it might serve as an indicator for the Pacific Winter Water layer because of its restricted depth distribution in the Chukchi Sea. We have also discussed the taxonomic position of the order Entactinaria and have emended

the genus *Joergensenium*. Our findings are based on quantitative and qualitative observations of shell morphology using a transmitted light microscope, a scanning electron microscope and Microfocus X-ray Computed Tomography. Micro-CT technology has been utilized for the first time in a species description and would be an effective tool for detailed observation of the internal structure of shell-bearing microplankton in the near future.

Supplementary data to this article can be found online at http://dx.doi.org/10.1016/j.marmicro.2016.02.003.

References

Aagaard, K., Coachman, L.K., Carmack, E., 1981. On the halocline of the Arctic Ocean. Deep Sea Res., Part I 28, 529–545.

Aagaard, K., Swift, J.H., Carmack, E.C., 1985. Thermohaline circulation in the Arctic Mediterranean seas. J. Geophys. Res. 90, 4833–4846.

Anderson, O.R., 1983. Radiolaria. Springer, New York (365 pp.).

Anderson, O.R., Nigrini, N., Boltovskoy, D., Takahashi, K., Swanberg, N., 2002. Class Polycystinea. In: Lee, J. (Ed.), An Illustrated Guide to the Protozoa, second ed. Society of Protozoologists, Lawrence, KS, pp. 994–1022.

Bjørklund, K.R., 1974a. The seasonal occurrence and depth zonation of radiolarians in Korsfjorden, Western Norway. Sarsia 56, 13–42.

Bjørklund, K.R., 1974b. A rare skeleton form in *Echinomma leptodermum* (Spumellaria, Radiolaria). Sarsia 56, 43–46.

Bjørklund, K.R., 1976. *Actinomma haysi*, n. sp., its Holocene distribution and size variation in Atlantic Ocean sediments. Micropaleontology 23, 114–126.

Bjørklund, K.R., Kruglikova, S.B., 2003. Polycystine radiolarians in surface sediments in the Arctic Ocean basins and marginal seas. Mar. Micropaleontol. 49, 231–273.

Bjørklund, K.R., Cortese, G., Swanberg, N., Schrader, H.J., 1998. Radiolarian faunal provinces in surface sediments of the Greenland, Iceland and Norwegian (GIN) seas. Mar. Micropaleontol. 35, 105–140.

Bjørklund, K.J., Dumitrica, P., Dolven, J.K., Swanberg, N.R., 2008. *Joergensenium rotatile* n. gen., n. sp. (Entactinaria, Radiolaria): its distribution in west Norwegian fjords. Micropaleontology 53, 457–468.

Blueford, J.R., 1983. Distribution of Quaternary radiolaria in the Navarin Basin geologic province, Bering Sea. Deep Sea Res. Part A 30, 763–781.

Boltovskoy, D., Kogan, M., Alder, V.A., Mianzan, H., 2003. First record of a brackish radiolarian (Polycystina): *Lophophaena rioplatensis* n. sp. in the Rio de la Plata estuary. J. Plankton Res. 25, 1551–1559.

Bråte, J., Krabberød, A.K., Dolven, J.K., Ose, R.F., Kristensen, T., Bjørklund, K.R., Shalchian-Tabrizi, Kamran, 2012. Radiolaria associated with large diversity of marine alveolates. Protist 163, 767–777.

Capella-Gutiérrez, S., Silla-Martínez, J.M., Gabaldón, T., 2009. trimAl: a tool for automated alignment trimming in large-scale phylogenetic analyses. Bioinformatics 25, 1972–1973.

Caron, D.A., Swanberg, N.R., 1990. The ecology of planktonic sarcodines. Aquatic Science 3. CRC Press, Boca Raton, FL, pp. 147–180.

Cavalier-Smith, T., 1999. Principles of protein and lipid targeting in secondary symbiogenesis: euglenoid, dinoflagellate, and sporozoan plastid origin and the eukaryote family tree. J. Eukaryot. Microbiol. 46, 347–366.

Cavalier-Smith, T., 2002. The phagotrophic origin of eukaryotes and phylogenetic classification of protozoa. Int. J. Syst. Evol. Microbiol. 52, 297–354.

Cavalier-Smith, T., 2003. Protist phylogeny and the high-level classification of protozoa. Eur. J. Protistol. 39, 338–348.

Ciesielski, P.F., Bjørklund, K.R., 1995. Ecology, morphology, stratigraphy, and the paleoceanographic significance of *Cycladophora davisiana*. Part II: stratigraphy in the North Atlantic (DSDP Site 609) and Labrador Sea (ODP Site 646B). Mar. Micropaleontol. 25, 67–86.

Coachman, L., Barnes, C.A., 1961. The contribution of Bering Sea water to the Arctic Ocean. Arctic 14, 147–161.

Comiso, J.C., 2012. Large decadal decline of the Arctic multiyear ice cover. J. Clim. 25, 1176–1193.

Cortese, G., Bjørklund, K.R., 1997. The morphometric variation of *Actinomma boreale* (Radiolaria) in Atlantic boreal waters. Mar. Micropaleontol. 29, 271–282.

Cortese, G., Bjørklund, K.R., Dolven, J.K., 2003. Polycystine radiolarians in the Greenland–Iceland–Norwegian seas: species and assemblage distribution. Sarsia 88, 65–88.

de Vargas, C., Audic, S., Henry, N., Decelle, J., Mahé, F., Logares, R., Lara, E., Berney, C., Le Bescot, N., Probert, I., Carmichael, M., Poulain, J., Romac, S., Colin, S., Aury, J.M., Bittner, L., Chaffron, S., Dunthorn, M., Engelen, S., Flegontova, O., Guidi, L., Horák, A., Jaillon, O., Lima-Mendez, G., Lukeš, J., Malviya, S., Morard, R., Mulot, M., Scalco, E., Siano, R., Vincent, F., Zingone, A., Dimier, C., Picheral, M., Searson, S., Kandels-Lewis, S., Coordinators, Tara Oceans, Acinas, S.G., Bork, P., Bowler, C., Gorsky, G., Grimsley, N., Hingamp, P., Iudicone, D., Not, F., Ogata, H., Pesant, S., Raes, J., Sieracki, M.E., Speich, S., Stemmann, L., Sunagawa, S., Weissenbach, J., Wincker, P., Karsenti, E., 2015. Eukaryotic plankton diversity in the sunlit ocean. Science 348, 6237. http://dx.doi.org/10.1126/science.1261605.

De Wever, P., Dumitrica, P., Caulet, J.P., Nigrini, C., Caridroit, M., 2001. Radiolarians in the Sedimentary Record. Gordon and Breach Science Publishers, Amsterdam (533 p.).

Dolven, J.K., 1998. Late Pleistocene to Late Holocene Biostratigraphy and Paleotemperatures in the SE Norwegian Sea, Based on Polycystine Radiolarians Master's Degree Thesis University of Oslo (Norway) (155 pp).

Dolven, J.K., Cortese, G., Bjørklund, K.R., 2002. A high-resolution radiolarian-derived paleotemperature record for the Late Pleistocene–Holocene in the Norwegian Sea. Paleoceanography 17, 1072. http://dx.doi.org/10.1029/2002PA000780.

Dolven, J.K., Lindqvist, C., Albert, V.A., Bjørklund, K.R., Yuasa, T., Takahashi, O., Mayama, S., 2007. Molecular diversity of alveolates associated with Neritic North Atlantic Radiolarians. Protist 158, 65–76.

Dumitrica, P., 1995. Systematic framework of Jurassic and Cretaceous Radiolaria. In: Baumgartner, P.O., O' Dogherty, L., Gorican, S., Pillevuit, A., De Wever, P. (Eds.), Middle Jurassic to Lower Cretaceous Radiolaria of Tethys: Occurrences, Systematics, Biochronology, 19–35. Mémoires de Géologie (Lausanne), p. 23.

Dumitrica, P., 2014. On the status of the radiolarian genera *Lonchosphaera Popofsky*, 1908 and *Arachnostylus* Hollande and Enjumet, 1960. Acta Palaeontol. Romaniae 9, 57–64.

Ehrenberg, C.G., 1839. Über die Bildung der Kreidefelsen und des Kreidemergels durch unsichtbare Organismen. Abhandl. der Konigl. Akad. der Wiss. zu Berlin, Jahrg. 1838, 59–147.

Environmental Working Group (EWG), 1998. Joint U.S. — Russian Atlas of the Arctic Ocean, Oceanography Atlas for the Winter Period. National Ocean Data Center (CD-ROM available from the National Snow and Ice Data Center (NSIDC), Boulder, CO).

Guillou, L., Viprey, M., Chambouvet, A., Welsh, R.M., Kirkham, A.R., Massana, R., Scanlan, D.J., Worden, A.Z., 2008. Widespread occurrence and genetic diversity of marine parasitoids belonging to Syndiniales (Alveolata). Environ. Microbiol. 10, 3349–3365.

Harada, N., 2016. Review: Potential catastrophic reduction of sea ice in the western Arctic Ocean: Its impact on biogeochemical cycles and marine ecosystems. Glob. Planet. Chang. 136, 1–17.

Ikenoue, T., Takahashi, K., Tanaka, S., 2012a. Fifteen year time-series of radiolarian fluxes and environmental conditions in the Bering Sea and the central subarctic Pacific, 1990–2005. Deep Sea Res., Part II 61–64, 17–49.

Ikenoue, T., Ueno, H., Takahashi, K., 2012b. *Rhizoplegma boreale* (Radiolaria): a tracer for mesoscale eddies from coastal areas. J. Geophys. Res. 117, C04001. http://dx.doi.org/10.1029/2011JC007728.

Ikenoue, T., Bjørklund, K.R., Kruglikova, S.B., Onodera, J., Kimoto, K., Harada, N., 2015. Flux variations and vertical distributions of siliceous Rhizaria (Radiolaria and Phaeodaria) in the western Arctic Ocean: indices of environmental changes. Biogeosciences 12, 2019–2046. http://dx.doi.org/10.5194/bg-12-2019-2015.

Itaki, T., Bjørklund, K.R., 2007. Conjoined radiolarian skeletons (Actinommidae) from the Japan Sea sediments. Micropaleontology 53, 371–389.

Itaki, T., Ito, M., Narita, H., Ahagon, M., Sakai, I., 2003. Depth distribution of radiolarians from the Chukchi and Beaufort Seas, western Arctic. Deep Sea Res., Part I 50, 1507–1522.

Jackson, J.M., Allen, S.E., McLaughlin, F.A., Woodgate, R.A., Carmack, E.C., 2011. Changes to the near surface waters in the Canada Basin, Arctic Ocean from 1993 to 2009: a basin in transition. J. Geophys. Res. 116, C10008. http://dx.doi.org/10.1029/2011JC007069.

Jones, E.P., Anderson, L.G., 1986. On the origin of the chemical properties of the Arctic Ocean halocline. J. Geophys. Res. 91, 10759–10767.

Katoh, K., Standley, D.M., 2013. MAFFT multiple sequence alignment software version 7: Improvements in performance and usability. Mol. Biol. Evol. 30, 772–780.

Kling, S.A., 1978. Radiolaria. In: Haq, B.U., Boersma, A. (Eds.), Introduction to Marine Micropaleontology. Elsevier, New York, pp. 203–244.

Kozur, H., Mostler, H., 1982. Entactinaria subordo nov., a new radiolarian suborder. Mitt. Geol. Paläontol. Innsbruck 11 (12), 399–414.

Krabberød, A.K., Bråte, J., Dolven, J.K., Ose, R.F., Klaveness, D., Kristensen, T., Bjørklund, K.R., Shalchian-Tabrizi, Kamran, 2011. Radiolaria divided into polycystina and Spasmaria in combined 18S and 28S rDNA phylogeny. PLoS One 6, e23526. http://dx.doi.org/10.1371/journal.pone.0023526.

Lee, K.E., Bahk, J.J., Narita, H., 2003. Temporal variations in productivity and planktonic ecological structure in the East Sea (Japan Sea) since the last glaciation. Geo-Mar. Lett. 23, 125–129.

McLaughlin, F.A., Carmack, E., Proshutinsky, A., Krishfield, R.A., Guay, C.K., Yamamoto-Kawai, M., Jackson, J.M., Williams, W.J., 2011. The rapid response of the Canada

Basin to climate forcing: From bellwether to alarm bells. Oceanography 24, 146–159. http://dx.doi.org/10.5670/oceanog.2011.66.

Melling, H., Lewis, E.L., 1982. Shelf drainage flows in the Beaufort Sea and their effect on the Arctic Ocean pycnocline. Deep Sea Res. Part A 29, 967–986.

Müller, J., 1859. Über die Thalassicollen, Polycystinen und Acanthometren des Mittelmeeres. Abhandl. der Konigl. Akad. der Wiss. zu Berlin, Jahrg. 1858, 1–62 (11 pls).

Nishino, S., 2013. R/V Mirai Cruise Report MR13-06 (226 pp., available at: www.godac. jamstec.go.jp/darwin/datatree/e (last access: 20 December 2015)) JAMSTEC, Yokosuka, Japan.

Not, F., Gausling, R., Azam, F., Heidelberg, J.F., Worden, A.Z., 2007. Vertical distribution of picoeukaryotic diversity in the Sargasso Sea. Environ. Microbiol. 9, 1233–1252.

Orr, R.J.S., Murray, S.A., Stüken, A., Rhodes, L., Jakobsen, K.S., 2012. When naked became armored: an eight-gene phylogeny reveals monophyletic origin of theca in dinoflagellates. PLoS One 7, e50004. http://dx.doi.org/10.1371/journal.pone.0050004.

Petrushevskaya, M.G., 1971. Radiolyarii Nassellaria v planktone Mirovogo Okeana. Issledovaniya Fauny Morei, Nauka, Leningrad, 9(17), (420 pp.).

Renaudie, J., Lazarus, D.B., 2015. New species of Neogene radiolarians from the Southern Ocean–part III. J. Micropalaeontol. 34, 181–209. http://dx.doi.org/10.1144/jmpaleo2013-034.

Reynolds, R.W., Rayner, N.A., Smith, T.M., Stokes, D.C., Wang, W., 2002. An improved in situ and satellite SST analysis for climate. J. Climate 15, 1609–1625.

Riedel, W.R., 1967. Subclass Radiolaria. In: Harland, W.B., Holland, C.H., House, M.R., Hughes, N.F., Reynolds, A.B., Rudwick, M.J.S., Satterthwaite, G.E., Tarlo, L.B.H., Willey, E.C. (Eds.), The fossil record. The Geological Society of London, pp. 291–298.

Skovgaard, A., 2014. Dirty tricks in the plankton: diversity and role of marine parasitic protists. Acta Protozool. 51–62.

Stamatakis, A., 2014. RAxML version 8: a tool for phylogenetic analysis and post-analysis of large phylogenies. Bioinformatics 2010–2011.

Stroeve, J.C., Serree, M.C., Holland, M.M., Kay, J.E., Malanik, J., Barrett, A.P., 2012. The Arctic's rapidly shrinking sea ice cover: a research synthesis. Clim. Chang. 110, 1005–1027.

Suzuki, N., Aita, Y., 2011. Achievement and unsolved issues on radiolarian studies: taxonomy and cytology. Plankon Benthos Res. 6, 69–91.

Tada, R., Irino, T., Koizumi, I., 1999. Land-ocean linkages over orbital and millennial timescales recorded in Late Quaternary sediments of the Japan Sea. Paleoceanography 14, 236–247.